XBAT31 regulates thermoresponsive hypocotyl growth through mediating degradation of the thermosensor ELF3 in Arabidopsis

Lin-Lin Zhang[1], Yu-Jian Shao[1], Lan Ding[1], Mei-Jing Wang[1], Seth Jon Davis[2,3] and Jian-Xiang Liu [1,*]

[1]State Key Laboratory of Plant Physiology and Biochemistry, College of Life Sciences, Zhejiang University, Hangzhou 310027, China.

[2]Department of Biology, University of York, Heslington, York, YO105DD, UK.

[3]State Key Laboratory of Crop Stress Biology, School of Life Sciences, Henan University, Kaifeng 475004, China.

[*]Correspondence：jianxiangliu@zju.edu.cn

Article type:

Full article

Short title:

XBAT31 controls ELF3 stability at warm temperature

One-sentence summary:

This paper reveals that XBAT31 ubiquitinates and degrades ELF3 to attenuate its inhibitory effects on PIF4.

ABSTRACT

Elevated ambient temperature has wide effects on plant growth and development. ELF3, a recently proposed thermosensor, negatively regulates protein activity of the growth-promoting factor PIF4, and such an inhibitory effect is subjected to attenuation at warm temperature. However, how ELF3 stability is regulated at warm temperature remains enigmatic. Here, we report the identification of XBAT31 as the E3 ligase that mediates ELF3 degradation in response to warm temperature in Arabidopsis. XBAT31 interacts with ELF3, ubiquitinates ELF3, and promotes ELF3 degradation via the 26S proteasome. Mutation of *XBAT31* results in enhanced accumulation of ELF3 and reduced hypocotyl elongation at warm temperature. In contrast, overexpression of *XBAT31* accelerates ELF3 degradation and promotes hypocotyl growth. Further, XBAT31 interacts with the B-box protein BBX18, and the XBAT31-mediated ELF3 degradation is dependent on *BBX18*. Thus, our findings reveal that XBAT31-mediated destruction of ELF3 represents an additional regulatory layer of complexity in temperature signalling during thermomorphogenesis in plants.

Keywords: XBAT31; ELF3; PIF4; BBX18; warm temperature; hypocotyl growth; thermomorphogenesis; ubiquitination; protein degradation

INTRODUCTION

Global temperature increases have had major negative impacts on plant ecosystem and the productivity of crop species (*1*). Plants are able to sense ambient temperature changes and adjust their growth and developmental programmes accordingly. In the model plant Arabidopsis, warm temperature alters growth, including hypocotyl elongation, leaf hyponasty, and accelerates flowering, in a process called thermomorphogenesis (*2*). Phytochromes, especially phyB, originally identified as photoreceptors, also function as thermosensors in Arabidopsis (*3-5*). Warm temperature accelerates the conversation of phyB from active Pfr back to inactive Pr, therefore releasing the inhibitory effects of phyB on PHYTOCHROME INTERACTING FACTOR (PIF) family proteins, such as the bHLH transcription factor PIF4 (*6*). PIF4 is a key regulator of plant thermomorphogenesis, which is subjected to various regulations both at transcriptional and post translational levels (*7-16*).

The evening complex (EC), consisting of EARLY FLOWERING3 (ELF3), EARLY FLOWERING4 (ELF4), and LUX ARRYTHMO (LUX), are core components of the circadian clock and coordinate environmental temperature cues with endogenous developmental signals for thermoresponsive gene expression and hypocotyl growth (*17*). ELF3 recruits ELF4 and LUX to repress the transcriptional expression of *PIF4* during early night (*12, 18*). ELF3 also suppresses PIF4 protein activity in an EC-independent manner by preventing PIF4 from activating its transcriptional targets in the light (*19*). ELF3 has a polyglutamine (polyQ) tract and changing the length of polyQ repeats affects ELF3-dependent phenotypes in a striking and nonlinear manner (*20*). Recently, the polyQ repeats of ELF3 within a predicted prion-like domain (PrD) were reported to function as a thermosensor in Arabidopsis (*21*). ELF3 PrD undergoes liquid-liquid phase separation, which releases the inhibitory effect of

ELF3 on PIF4 under warm temperature conditions (*21*), however, how the protein stability of ELF3 is controlled at warm temperature remains enigmatic.

The B-box (BBX) family proteins are zinc-finger proteins of which the BBX motif is important for transcriptional regulation and protein-protein interactions (*22*). Recently, group IV BBX proteins BBX18 and BBX23 were identified to be involved in plant thermomorphogenesis through regulating the protein abundance of ELF3 (*23*). Although CONSTITUTIVE PHOTOMORPHOGENIC1 (COP1), an E3 ubiquitin ligase known to be involved in controlling ELF3 stability in the photoperiod pathway under normal temperature conditions, interacts with BBX18 and BBX23, the level of ELF3 was not found to be further increased in the *cop1-4* mutant at warm temperature, suggesting that other E3 ligases existed to regulate ELF3 degradation during plant thermomorphogenesis (*23, 24*). In this study, we demonstrate that XB3 ORTHOLOG 1 IN ARABIDOPSIS THALIANA, XBAT31, regulates ELF3 stability at warm temperature. Our results show that XBAT31 is a positive thermomorphogenesis regulator that interacts with ELF3, ubiquitinates ELF3, and this leads to ELF3 degradation at warmer temperature. Interestingly, full XBAT31-mediated ELF3 degradation requires the previous identified thermomorphogenesis regulator BBX18. Therefore, our findings reveal an important mechanism in which ELF3 is modulated at the protein level by XBAT31 in response to elevated ambient temperature.

RESULTS

XBAT31 regulates hypocotyl elongation at warm temperature

In our previous RNA-Seq analysis of thermoresponsive gene expression in Arabidopsis (*23*), we identified a putative E3 ubiquitin protein ligase, *XBAT31* (AT2G28840), that is up-regulated by warm temperature. XBAT31 is one of the five Arabidopsis gene products structurally related to XA21 BINDING PROTEIN3 (XB3) in rice (*25-29*), but its function in plants has not yet been characterized.

There are two splicing isoforms of *XBAT31* in the TAIR database, *XBAT31.1* and *XBAT31.2*, with *XBAT31.1* containing an additional exon. To determine which form is responsive to warm temperature, we carried out quantitative RT-PCR (RT-qPCR) in wild-type (WT) plants under conditions of normal (22°C) and warm (29°C) ambient temperatures, respectively. Compared with the expression level at normal growth temperature, the expression of *XBAT31.1*, but not *XBAT31.2*, was increased by warm temperature (**Fig. 1A-B**). Therefore, we focused on *XBAT31.1* in later studies. The thermoresponsive increases in *XBAT31* was not dependent on *PIF4* or *BBX18*/*BBX23* (*23*). We next checked the expression of *XBAT31* in phyA and phyB mutants, which are reported to function as thermosensors for hypocotyl growth (*3, 4*). Compared with the WT, mutation at either *PHYA* or *PHYB* or both did not significantly affect the warm temperature-induced up-regulation of *XBAT31* (**Fig. S1**). Thus, *XBAT31* expression is responsive to warm temperature independent of *PHYA*/*PHYB*.

To understand the biological function of *XBAT31* in plant thermomorphogenesis, we generated several independent loss-of-function mutant lines of *XBAT31* with the CRISPR-Cas9 targeted gene editing system (**Fig. S2**), and two of them were used for measurements of hypocotyl length, a phenotypic trait that is highly responsive to warm temperature. These mutants

grew normally at the seedling stage and had a similar hypocotyl length as the WT plants under normal ambient growth temperature conditions in the light (**Fig. 1C-D**), as well as in the dark (**Fig. S3A & S3C**). However, compared with that of the WT seedlings, the hypocotyl length was significantly reduced in both lines of *XBAT31* mutants at warm temperature (**Fig. 1C-D**). We next generated *XBAT31* overexpression plants using the constitutive CaMV 35S promoter (**Fig. S4A**). The hypocotyl length of the overexpression plants was measured and was similar to that of the WT plants in the dark (**Fig. S3B & S3D**) and slightly longer than that in the WT plants under the light when grown at 22°C (**Fig. 1E-F**). In contrast, at warm temperature (29°C), the hypocotyl length of *XBAT31* overexpression plants was much longer than that of the WT (**Fig. 1E-F**). Therefore, XBAT31 is an important positive regulator in thermomorphogenesis in Arabidopsis.

Plant thermomorphogenesis often relies on transcriptional regulation of gene expression involved in phytohormone biosynthesis and signalling (*8, 9, 30, 31*). To further understand whether XBAT31 controls the expression of thermoresponsive genes, we compared the expression of three auxin responsive marker genes, *YUCCA8* (*YUC8*), *INDOLE-3-ACETIC ACID INDUCIBLE19* (*IAA19*), and *F-box family protein* (*AT1G73120*) (*23*), in the WT, *xbat31-1* mutant, and *XBAT31ox-1* overexpression plants. This was performed under both normal and warm temperature conditions. We found that all these three genes showed increased transcript accumulation in warm temperature in the WT plants at ZT 8 hr and ZT 24 hr. However, *YUC8* displayed a lower increase, and the other two genes were not increased at warm temperature in *xbat31-1* mutant plants at ZT 8 hr. In contrast, the expression of all these three genes was elevated by warm temperature in *XBAT31ox-1* overexpression plants than that in WT plants at ZT 8 hr and ZT 24 hr (**Fig. 1G-H**). We also checked the gene expression of *ELF3* and *PIF4*, two important genes regulating

147 plant thermomorphogenesis. The expression of both in *xbat31-1* or *XBAT31ox-*
148 *1* plants was similar to that of WT plants under both temperature conditions (**Fig.**
149 **S5**). Taken together, our results demonstrate that XBAT31 is an important
150 positive regulator of plant thermomorphogenesis.
151
152 ***XBAT31* functions upstream of *PIF4* in the thermomorphogenesis**
153 **pathway**
154 It is well established that the bHLH transcription factor PIF4 is a hub for ambient
155 temperature responses that integrates various environmental signals into plant
156 morphogenesis and growth control (*2*). To analyze the genetic relationship
157 between *XBAT31* and *PIF4*, we examined the hypocotyl phenotype of single
158 mutants of *XBAT31* and *PIF4*, as well as double mutant plants under normal
159 and warm temperature conditions. The hypocotyls of *xbat31-1 pif4-101* plants
160 did not elongate at 29°C as much as the *pif4-101* single mutant (**Fig. 2A & 2D**).
161 Thus, *PIF4* is epistatic to *XBAT31*. To determine whether the function of
162 XBAT31 in thermomorphogenesis depends on *PIF4*, we overexpressed
163 *XBAT31* in both the WT and *pif4-101* mutant backgrounds, obtained through
164 genetic crossing (**Fig. S4B**). As shown above, *XBAT31* overexpression in the
165 WT background conferred an elevated thermoresponsive hypocotyl-growth
166 phenotype compared to the WT. However, in the *PIF4* mutant background,
167 *XBAT31* overexpression plants had a similar hypocotyl length as the *pif4-101*
168 mutant plants (**Fig. 2B & 2E**). Therefore we concluded that the function of
169 XBAT31 in hypocotyl growth is dependent on *PIF4*. Overexpression of *PIF4* in
170 the WT background enhances hypocotyl elongation (*14, 23, 32*). We crossed
171 the *PIF4* overexpression plants to the *XBAT31* mutant plants (**Fig. S4C**) and
172 checked the thermoresponsive hypocotyl phenotypes. As expected, *PIF4*
173 overexpression promoted hypocotyl elongation in both the WT and *XBAT31*

mutant backgrounds (**Fig. 2C & 2F**). Taken together, these results support that *XBAT31* functions upstream of *PIF4* in thermomorphogenesis.

***ELF3* is epistatic to *XBAT31* during thermomorphogenesis**

ELF3 is a key component of the EC, and the EC regulates its targets in a temperature dependent fashion (*12*). One of the key EC targets is the gene *PIF4* that along with all the other EC targets becomes more highly expressed at high temperature because ELF3 responds to temperature, inactivating the EC (*33, 34*). Separately, it appears that ELF3 also binds and inhibits the activity of the PIF4 protein from activating its transcriptional targets (*19*). We were thus interested in exploring the genetic relationship of *XBAT31* and *ELF3*. Compared with the WT, *elf3-101* mutant plants had longer hypocotyls whereas *xbat31-1* mutant plants had shorter hypocotyls at 29°C (**Fig. 2G & 2I**). However, the *ELF3* and *XBAT31* double mutant *xbat31-1 elf3-101* plants resembled the *elf3-101* single mutant plants in terms of hypocotyl elongation (**Fig. 2G & 2I**), which supports that *ELF3* is epistatic to *XBAT31* during thermomorphogenesis. We also generated *XBAT31* and *ELF3* double overexpression plants by crossing the *XBAT31ox-1* plants and *ELF3*ox-1 plants, in which *XBAT31* and *ELF3* were overexpressed under the control of the CaMV 35S promoter (**Fig. S4D**). *ELF3* overexpression suppressed hypocotyl elongation while *XBAT31* overexpression promoted hypocotyl elongation at 29°C (**Fig. 2H & 2J**). However, the hypocotyl length of the *ELF3*ox-1 *XBAT31*ox-1 double overexpression plants was similar to that of the *XBAT31*ox-1 single overexpression plants under both normal and warm temperature conditions (**Fig. 2H & 2J**). These results suggest that the function of XBAT31 in thermomorphogenesis is dependent on ELF3, and ELF3 probably is an *in vivo* target of XBAT31 during hypocotyl growth.

XBAT31 interacts with ELF3 both *in vitro* and *in vivo*

To better understand the relationship between XBAT31 and ELF3, we next tested for their possible protein-protein interaction in the yeast two-hybrid assay. Initial results showed that XBAT31 interacted with ELF3 in yeast cells, subsequently we made four truncations (F1-F4) for XBAT31 and three truncations (N, M, and C) for ELF3, respectively, to further narrow down the interaction sites (**Fig. 3A-B**). It was found that the region (P301-P361) containing the RING finger domain of XBAT31 was sufficient to interact with ELF3, and both the N-terminal and middle domains of ELF3 could interact with XBAT31 (**Fig. 3C-D**).

The interactions between XBAT31 and ELF3 were confirmed by further assays. In *in vitro* pull-down assays, the glutathione S-transferase (GST)-tagged ELF3 precipitated with the maltose binding protein (MBP)-tagged XBAT31 (**Fig. 3E**). By using split-luciferase assays and split-YFP assays in *Nicotiana benthamiana* leaves, we confirmed the occurrence of interaction between XBAT31 and ELF3 in plants (**Fig. 3F-G**). The XBAT31-YFP fusion protein was observed in nucleus (**Fig. S6**), and the interaction between XBAT31 and ELF3 was also found in nucleus in the split-YFP assays (**Fig. 3G**). We next performed co-immunoprecipitation (Co-IP) assays in Arabidopsis, and the results showed that the FLAG-tagged XBAT31 could be co-immunoprecipitated with the endogenous ELF3 (**Fig. 3H**). Taken together, our results demonstrate that XBAT31 interacts with ELF3 both *in vitro* and *in vivo*.

XBAT31 mediates the ubiquitination and degradation of ELF3

As ELF3 is a protein that interacts with the ubiquitin E3 ligase XBAT31, we speculated that XBAT31 may negatively regulate the stability of ELF3 by mediating its ubiquitination and degradation. To examine whether XBAT31 promotes this proteolysis of ELF3, we performed cell-free degradation assay

with extracts from the WT and *XBAT31* overexpression plants, respectively. Our results showed that ELF3 degradation was faster in *XBAT31ox-1* plants than that in WT plants. This ELF3 degradation was inhibited by MG132, an inhibitor of the 26S proteasome degradation system (**Fig. 4A-D**). Thus, XBAT31 promotes ELF3 degradation in a manner dependent on the 26S proteasome.

To investigate whether the E3 ligase XBAT31 facilitates ELF3 degradation directly by ubiquitination, *in vitro* ubiquitination assays were performed. GST-ELF3 and MBP-XBAT31 were purified from *E. coli* and incubated in the presence or absence of E1 (UBA1), E2 (UBCh5b) and ubiquitin (Ub). A version of XBAT31 (MBP-XBAT31M) in which the RING domain of XBAT31 was mutated (H336A) was also included. Our results showed that the native form MBP-XBAT31, but not the mutated form MBP-XBAT31M, was auto-ubiquitinated as detected by using the *anti*-Ub antibody (**Fig. 4E**). It was difficult to differentiate the auto-ubiquitinated XBAT31 and ubiquitinated ELF3 on gels with *anti*-Ub antibody, however, GST-ELF3 was conjugated with ubiquitin molecules in the presence of ubiquitin, E1, E2 and MBP-XBAT31 as shown with the *anti*-GST or *anti*-ELF3 antibody (**Fig. 4E**). In contrast, the mutated form of XBAT31 (H336A) could not ubiquitinate ELF3 under the same reaction conditions (**Fig. 4E**). All above biochemical results demonstrate that XBAT31 can lead to ubiquitination of ELF3, which is dependent on the RING domain of XBAT31.

To understand how XBAT31 regulates the protein stability of ELF3 in Arabidopsis plants during thermomorphogenesis, we examined ELF3 protein levels by western blotting with ELF3-specific antibody (**Fig. S4G**) in *XBAT31* mutant and overexpression plants under both normal and warm temperatures, respectively. Since the warm temperature-induced hypocotyl elongation was more prominent during the daytime under long-day conditions (*35*), and differential expression of thermoresponsive marker genes between WT and

XBAT31 mutant or overexpression plants was observed at ZT 8 hr (**Fig. 1G-H**), we collected protein extracts at ZT 8 hr and performed western-blotting analysis. We found lower levels of ELF3 in the warm temperature when comparing with that at normal growth temperature in the WT (**Fig. 4F-I**). Furthermore, the protein level of ELF3 was lower in *XBAT31* overexpression plants than that in WT under both temperature conditions (**Fig. 4F & 4H**). In contrast, unlike that in the WT, the ELF3 protein level was not reduced by warm temperature in the *XBAT31* mutant plants (**Fig. 4G & 4I**). Taken together, our results support that XBAT31 mediates the ubiquitination and degradation of ELF3 at warm temperature.

XBAT31-mediated thermomorphogenesis requires BBX18

Previously, we have shown that the B-box family proteins BBX18 and BBX23 regulate ELF3 stability during thermomorphogenesis, and that the E3 ubiquitin ligase COP1 plays only a minor role in mediating ELF3 degradation at warm temperature (*23*). Therefore, we were interested in whether the function of XBAT31 in thermomorphogenesis depends on BBX18/BBX23. We crossed the *XBAT31* overexpression plants with the *BBX18* single mutant, or the *BBX23* single mutant, or the double mutant *bbx18-1 bbx23-1* (**Fig. S4E-F**), and checked their hypocotyl growth under normal and warm temperature conditions. As reported above, overexpression of *XBAT31* in the WT background accelerated hypocotyl elongation. However, the hypocotyl phenotype was suppressed in either the *bbx18-1* single mutant background or in the *bbx18-1 bbx23-1* double mutant background, but not in the *bbx23-1* single mutant background, both at normal and warm temperatures (**Fig. 5A-E**). Our results revealed that the function of XBAT31 in thermomorphogenesis is dependent on BBX18. We also crossed *xbat31-1* mutant to *bbx18-1* mutant and generated the *xbat31-1 bbx18-1* double mutant, and the phenotypic analysis showed that

hypocotyl length of the *xbat31-1 bbx18-1* double mutant is similar to that of the *xbat31-1* mutant or the *bbx18-1* mutant plants (**Fig. 5F**). These results demonstrated that XBAT31 and BBX18 function in thermomorphogenesis in the same regulatory pathway.

To test for a possible physical interaction between XBAT31 and BBX18, we performed *in vitro* pull-down assays. Our results showed that GST-XBAT31 was able to pull down MBP-BBX18 (**Fig. 5G**). Split-luciferase assays and split-YFP assays further confirmed the occurrence of interaction between XBAT31 and BBX18 in plants (**Fig. 5H-I**). We also checked the ELF3 protein levels at ZT 8 hr in *XBAT31* overexpression plants in the WT and *bbx18* mutant backgrounds. As expected, the protein level of ELF3 under warm temperature conditions was higher in the *bbx18-1* mutant plants compared with that in the WT plants at ZT 8 hr (**Fig. 5J & 5L**), and the accumulation of ELF3 in the *bbx18-1* mutant background was much higher than that in the WT background when *XBAT31* was overexpressed (**Fig. 5K & 5M**). The ELF3 protein level was higher in the *bbx18-1* mutant background than that in the WT background at 22°C, possibly because BBX18 also has other function at normal growth temperature when XBAT31 is overexpressed. We conclude that XBAT31-mediated degradation of ELF3 at warm temperature depends on the function of BBX18 in Arabidopsis.

DISCUSSION

Sensing prevailing temperature helps plant to better adapt to the surrounding environment. Both warm temperature and reduced light conditions promote hypocotyl elongation, leaf hyponasty and early flowering. There are multiple perception points that signal thermal changes. phyB is the main photoreceptor with two different activation states (*36*). Warm temperature controls the conversion of phyB from the active Pfr state to the inactive Pr state, releasing the inhibitory effect of phyB on PIF4 (*3, 4*). In contrast, ELF3 functions in

Arabidopsis through a differing mechanism in which warm temperature induces liquid-liquid phase separation of ELF3, leading to its inactivation and therefore activation of PIF4 at a warm temperature (*21*). In the current study, we demonstrate that the E3 ubiquitin ligase XBAT31 controls the protein stability of ELF3, especially under warm temperature conditions. Interestingly, XBAT31-mediated thermomorphogenesis requires BBX18, a B-box family protein that responds to warm temperature both at transcriptional and post translational levels (*23*). These results provide new insights into our understanding on how warm temperature conveys the signal to ELF3 for hypocotyl growth in plants.

The EC is a night transcriptional repressor complex that functions in the plant circadian clock as well as in temperature and light entrainment (*12, 37, 38*). Among the three core components, only LUX has DNA-binding domain and directly binds to target DNA whereas ELF3 and ELF4 enhance the binding of EC to DNA (*39*). The EC represses the expression of *PIF4*, which is reduced by warm temperature (*12*). At warm temperature, the function of ELF4 on hypocotyl growth is dependent on *ELF3*, while overexpression of *ELF3* in *elf4-2* mutant background does not change thermal responsiveness, suggesting that these two proteins function together during thermomorphogenesis (*21*). However, ELF3 was also reported to function alone to inhibit the protein activity of PIF4, in which warm temperature releases such inhibitory effects (*19*). Genetic association studies showed that natural variation in *ELF3* locus is correlated with warm temperature-induced hypocotyl elongation in Arabidopsis, supporting the role of ELF3 in controlling PIF4 activity (*33, 34*). Our results showed that *XBAT31* functions upstream of *PIF4* and finely tunes the protein level of ELF3 at warm temperature. Therefore, XBAT31 regulates hypocotyl growth through releasing the inhibitory effects of ELF3 on PIF4 protein activity. We do not exclude the possibility that XBAT31 regulates thermomorphogenesis by affecting EC, since depletion of ELF3 would affect the entire EC. The

expression level of *PIF4* was not dramatically affected in *XBAT31* mutant and overexpression plants in our experiments, which was probably due to the long-day conditions used in the current study.

Under normal ambient temperature conditions, ELF3 is degraded by the E3 ligase COP1 in the dark, and light diminishes the abundance of COP1 and abrogates its inhibitory effects on ELF3 and other targets to promote photomorphogenesis (*24*). However, warm temperature triggers the nuclear import of COP1 and alleviates the suppression of hypocotyl elongation by degrading ELONGATED HYPOCOTYL5 (HY5) (*35*). Both the *ELF3* transcript expression and ELF3 protein accumulation were higher at ZT 24 hr at warm temperature than that at normal ambient temperature (*23*). Although BBX18/BBX23 enhanced COP1-mediated degradation of ELF3 in the effector-reporter assays in tobacco leaves, mutation of *COP1* did not while mutations of *BBX18*/*BBX23* did dramatically affect ELF3 accumulation during night time in Arabidopsis at warm temperature (*23*). In contrast, the *ELF3* transcriptional level was not changed while ELF3 protein level decreased at ZT 8 hr under light at warm temperature, and mutation of *XBAT31* were found to stabilize ELF3 accumulation at warm temperature, while overexpression of *XBAT31* accelerated ELF3 degradation in daytime under long-day conditions, which was dependent on the function of BBX18. Therefore, XBAT31 plays a major role in controlling ELF3 stability under light at warm temperature. We do not exclude the possibility that XBAT31 and BBX18/BBX23 also function at normal ambient growth temperature, since overexpression of *XBAT31* promotes hypocotyl growth to a small extent at 22°C.

How do XBAT31 and BBX18 respond to warm ambient temperature? The expressions of both *XBAT31* and *BBX18* were increased, while the protein level of XBAT31 was not obviously affected by warm temperature. In contrast, BBX18 protein was significantly stabilized by warm temperature (*23*). Therefore,

warm temperature may also convey signals to XBAT31 via BBX18. BBX18 belongs to the group IV BBX proteins that have two BBX motifs, but lacks the CONSTANS, CO-like, and TOC1 (CCT) domain essential for the DNA-binding activity in transcriptional regulation (*22, 40*). Although XBAT31 directly interacts with ELF3, BBX18 may function as a secondary scaffold protein to enhance the interaction between XBAT31 and ELF3 *in vivo* at warm temperature. It is not clear how warm temperature regulates the stability of BBX18, but our results indicate a central role of XBAT31 in transducing warm temperature signals from BBX18 and perhaps other BBX proteins to PIF4 in plants.

In summary, as depicted in the proposed model (**Fig. 6**), XBAT31 functions as a positive thermomorphogenesis regulator through regulating the protein stability of ELF3 in Arabidopsis. Under normal ambient growth temperatures, ELF3 suppresses PIF4 activity to inhibit hypocotyl elongation. In response to warm temperatures, both XBAT31 and BBX18 accumulate and function together to target ELF3 for 26S proteasome-associated degradation. This enables/enhances PIF4 to promote the expression of downstream genes for hypocotyl elongation, such as *YUC8*. This defines XBAT31 and BBX18 as upstream regulators for thermoresponsive hypocotyl growth.

MATERIALS AND METHODS

Plant materials and hypocotyl length measurements

Plants in the Columbia-0 (Col-0) background were used in the current study. Information on *pif4-101*, *elf3-101*, *bbx18-1*, *bbx23-1*, *PIF4ox-1* and *ELF3ox-1* plants was described in our previous paper (*23*). Seeds were surface-sterilized with 75% ethanol for 1 min and then with 0.01% sodium hypochlorite solutions for 20 min, and subsequently washed with sterilized water. All the seeds were grown directly on half-strength Murashige and Skoog (MS) medium (containing 1.2% sucrose and 0.6% agar, pH adjusted to 5.7), stratified at 4°C for 4 days,

and then transferred to a standard plant incubator with the following settings: 22°C, 16/8-hr day/night.

Independent lines of *XBAT31* loss-of-function mutants were generated using the CRISPR/Cas9 system (*41*). For overexpression of *XBAT31*, the coding sequences (CDS) of *XBAT31.1* were amplified and inserted into pCambia1306 with the 35S promoter. Primers are included in Table S1. The constructs were transformed into *Agrobacterium tumefaciens* strain GV3101 via the freeze-thaw method and introduced into Arabidopsis plants via the floral-dip method (*42*). Double mutants, double overexpression plants, and other materials as mentioned were obtained by crossing the respective parents and selecting for the appropriate segregant in the F2 generation.

For hypocotyl length measurements, when comparing the mutant plants with the wild-type (WT) plants, seedlings were grown at 22°C for 3 days, and then transferred to 29°C or maintained at 22°C for another 4 days; when comparing the overexpression plants with the WT plants, seedlings were grown at 22°C for 4 days, and then transferred to 29°C or maintained at 22°C for another 3 days. Seedlings were photographed by a camera, and the hypocotyl lengths were quantified using ImageJ software (National Institutes of Health). We used 24 seedlings from three biological replicates for these measurements. One-way ANOVA analyses and Tukey's honestly significant difference (HSD) test ($P < 0.05$) were performed for statistical analysis of the phenotypes.

Yeast two-hybrid assays

Full-length CDS and truncations of *ELF3*, *BBX18*, and *XBAT31* were cloned into pGADT7 (Clontech, Palo Alto, CA, USA) or pGBKT7 (Clontech) vectors to generate the baits and preys, respectively. Different combinations were co-transformed into yeast strain Y2HGold (Clontech) using a commercial kit (Zymo Research, Irvine, CA, USA) and grew on selective plates at 30°C for 2-4 days. All the primers are listed in Table S1.

Pull-down and Co-IP assays

Full-length CDS of *BBX18*, *ELF3*, and *XBAT31* was cloned into pETMALc-H, or pGEX4T-1 vectors to generate MBP-BBX18, GST-ELF3, MBP-XBAT31, or GST-XBAT31 fusion proteins. Transetta cells (Novagen, Madison, WI, USA) transformed with different respective vectors were induced by 300 μM isopropyl β-D-1-thiogalactopyranoside (IPTG) at 16°C overnight, and the resultant fusion proteins were affinity-purified with either amylose agarose beads (BioLabs, London, UK) or Glutathione-Super-flow resin (Takara, Japan), respectively, for MBP- and GST-tagged proteins. For pull-down assays, different combinations of recombinant proteins were incubated in pull-down buffer (20 mM Tris-HCl (pH 7.4), 200 mM NaCl, 1 mM EDTA) for 2 hr at 4°C with slow rotations. Subsequently, the beads were washed with pull-down buffer 3-5 times, and boiled with 2X SDS loading buffer. Protein extracts were separated in 4-20% SDS-PAGE gels and analyzed via *anti*-MBP (GenScrip, Piscataway, NJ, USA) or *anti*-GST (Abmart, Shanghai, China). For Co-IP assays, total proteins were extracted from WT and *XBAT31-FLAG* overexpression plants and immunoprecipitated with beads conjugated with *anti*-FLAG antibody (GenScript). After washing three times, beads were boiled with 2X SDS loading buffer and western blotting was performed with *anti*-ELF3 antibody (ABclonal, Wuhan, China). All the primers are listed in Table S1.

Split-luciferase and split-YFP assays

Full-length CDS of *ELF3*, *BBX18*, and *XBAT31* was fused in frame with the nLUC or cLUC (*23*) to generate cLUC-ELF3, cLUC-BBX18, or XBAT31-nLUC. Alternatively, they were fused to the nYFP or cYFP to generate nYFP-ELF3, nYFP-BBX18, or XBAT31-cYFP. Different combinations were transformed into *Agrobacterium tumefaciens* strain GV3101 and infiltrated into *Nicotiana benthamiana* leaves together with P19. Luciferase luminescence was detected by a Tanon 5200 Image Analyzer (Tanon, Shanghai, China). The YFP

fluorescence signals were detected under a confocal microscope LSM710NLO (Zeiss, Oberkochen, German). All the primers are listed in Table S1.

In vitro ubiquitination assays

Full-length CDS of *ELF3*, *XBAT31*, E1 (Arabidopsis *UBA1*), E2 (human *UBCH5b*), and Ub (*UBQ14*) were respectively cloned into pETMALc-H, pET-SUMO, or pGEX4T-1 vectors to generate GST-ELF3, MBP-XBAT31, MBP-XBAT31M, His-E1, His-E2, or His-E3 constructs that generate fusion proteins. A mutated form of XBAT31 in the RING domain (MBP-XBAT31M, H336A) was created by overlapping PCR. These fusion proteins, as well as MBP empty control, were purified with amylose agarose (BioLabs), Ni-NTA agarose (Qiagen, Berlin, Germany), or Glutathione-Super-flow resin (Takara), respectively. Ubiquitination assays were performed in reaction buffer containing 50 mM Tris-HCl (pH 7.5), 20 mM ZnCl2, 5 mM MgCl2, 2 mM ATP, 2 mM DTT and 20 μM MG132. After 2 hr incubation at 30°C, the reaction was stopped by adding SDS loading buffer. Ubiquitinated GST-ELF3 was detected by using *anti*-Ub (Santa Cruz Biotechnology, Dallas, TX, USA), *anti*-GST (Abmart) and *anti*-ELF3 (ABclonal) antibodies, respectively.

Cell-free degradation assay

WT and *XBAT31ox-1* plants grown at 22°C under LDs for 4 days were transferred to 29°C for 3 days and sampled at ZT 8 hr. Seedlings were harvested and total proteins were extracted using the extraction buffer (50 mM Tris-MES (pH 8.0), 0.5 mM sucrose, 1 mM MgCl2, 10 mM EDTA, 5mM DTT) with freshly added protease inhibitor cocktail CompleteMini tablets (Roche, Shanghai, China). After that the protein mixtures were incubated with 10 mM ATP and 50 μM Cycloheximide (CHX) at 29°C for 0-100 min in the presence or absence of 50 μM MG132. After SDS-PAGE, the abundance of ELF3 was detected by western blotting. Three independent experiments were performed and each immunoblot was quantified using ImageJ software.

Western blot analysis

To analysis the ELF3 protein levels in WT, *XBAT31ox-1*, *xbat31-1*, *bbx18-1* plants, or the multiple mutant genotypes, seedlings grown at 22 °C under LDs for 5 days were transferred to 29°C or maintained at 22°C for 24 hr and then sampled at ZT 8 hr. Total proteins were extracted with the extraction buffer (125 mM Tris-HCl (pH 8.0), 375 mM NaCl, 2.5 mM EDTA, 1% SDS and 1% β-mercaptoethanol), Afterward, the proteins were separated in 10% SDS-PAGE gels and analyzed using *anti*-ELF3 (*12, 19*) (ABclonal, Wuhan, China) and *anti*-tubulin (Sigma, Shanghai, China) antibodies. Three independent experiments were performed and each immunoblot was quantified using ImageJ software.

RT-qPCR

For reverse transcription-quantitative real-time polymerase chain reaction (RT-qPCR) analyses, 5-day-old seedlings grown at 22°C under LDs were transferred to 29°C or maintained at 22°C for 24 hr and then sampled at ZT 8, 16, 24 hr on the next day. Total RNAs were extracted with an RNA Prep Pure Plant kit (Tiangen, Shanghai, China). To synthesize cDNA, 2 μg of RNA and oligo (dT) primers were used in a 20-μL reaction using M-MLV reverse transcriptase (Invitrogen, Carlsbad, CA, USA). RT-qPCR was performed with SuperReal PreMix Color (Tiangen, Shanghai, China) in accordance with the manufacturer's protocol in a CFX96 real-time system (Bio-Rad, Hercules, CA, USA). The PCR programme was set as follows: first cycle, 95°C for 15 min; 40 cycles of denaturing (90°C for 10 sec), annealing (60°C for 30 sec), extension (72°C for 30 sec); last extension, 65°C to 95°C for 5 sec with an increment of 0.5°C. The expression level was calculated using the ΔΔCT method. There are three biological replicates in each experiment, and the expression of each gene was normalized to that of the reference gene *PP2A*. All the primers used are listed in Table S1.

REFERENCES

1. D. B. Lobell, W. Schlenker, J. Costa-Roberts, Climate trends and global crop production since 1980. *Science* **333**, 616-620 (2011).
2. M. Quint, C. Delker, K. A. Franklin, P. A. Wigge, K. J. Halliday, M. van Zanten, Molecular and genetic control of plant thermomorphogenesis. *Nat. Plant.* **2**, 15190 (2016).
3. J. H. Jung, M. Domijan, C. Klose, S. Biswas, D. Ezer, M. Gao, A. K. Khattak, M. S. Box, V. Charoensawan, S. Cortijo, M. Kumar, A. Grant, J. C. W. Locke, E. Schaefer, K. E. Jaeger, P. A. Wigge, Phytochromes function as thermosensors in Arabidopsis. *Science* **354**, 886-889 (2016).
4. M. Legris, C. Klose, E. S. Burgie, C. C. Rojas, M. Neme, A. Hiltbrunner, P. A. Wigge, E. Schafer, R. D. Vierstra, J. J. Casal, Phytochrome B integrates light and temperature signals in Arabidopsis. *Science* **354**, 897-900 (2016).
5. Y. Qiu, M. Li, R. J. Kim, C. M. Moore, M. Chen, Daytime temperature is sensed by phytochrome B in Arabidopsis through a transcriptional activator HEMERA. *Nat. Commun.* **10**, 140 (2019).
6. K. J. Halliday, S. J. Davis, Light-sensing phytochromes feel the heat. *Science* **354**, 832-833 (2016).
7. M. A. Koini, L. Alvey, T. Allen, C. A. Tilley, N. P. Harberd, G. C. Whitelam, K. A. Franklin, High temperature-medated adaptations in plant architecture require the bHLH transcription factor PIF4. *Curr. Biol.* **19**, 408-413 (2009).
8. K. A. Franklin, S. H. Lee, D. Patel, S. V. Kumar, A. K. Spartz, C. Gu, S. Ye, P. Yu, G. Breen, J. D. Cohen, P. A. Wigge, W. M. Gray, PHYTOCHROME-INTERACTING FACTOR 4 (PIF4) regulates auxin biosynthesis at high temperature. *Proc. Natl. Acad. Sci. USA* **108**, 20231-20235 (2011).
9. J. Sun, L. Qi, Y. Li, J. Chu, C. Li, PIF4-mediated activation of *YUCCA8* expression integrates temperature into the auxin pathway in regulating Arabidopsis hypocotyl growth. *PLOS Genet.* **8**, e1002594 (2012).
10. M. C. G. Proveniers, M. van Zanten, High temperature acclimation through PIF4 signaling. *Trend. Plant Sci.* **18**, 59-64 (2013).
11. S. V. Kumar, D. Lucyshyn, K. E. Jaeger, E. Alos, E. Alvey, N. P. Harberd, P. A. Wigge, Transcription factor PIF4 controls the thermosensory activation of flowering. *Nature* **484**, 242-245 (2012).
12. D. A. Nusinow, A. Helfer, E. E. Hamilton, J. J. King, T. Imaizumi, T. F. Schultz, E. M. Farre, S. A. Kay, The ELF4-ELF3-LUX complex links the circadian clock to diurnal control of hypocotyl growth. *Nature* **475**, 398-402 (2011).
13. C. Delker, L. Sonntag, G. V. James, P. Janitza, C. Ibanez, H. Ziermann, T. Peterson, K. Denk, S. Mull, J. Ziegler, S. J. Davis, K. Schneeberger,

M. Quint, The DET1-COP1-HY5 pathway constitutes a multipurpose signaling module regulating plant photomorphogenesis and thermomorphogenesis. *Cell Rep.* **9**, 1983-1989 (2014).
14. D. Ma, X. Li, Y. Guo, J. Chu, S. Fang, C. Yan, J. P. Noel, H. Liu, Cryptochrome 1 interacts with PIF4 to regulate high temperature-mediated hypocotyl elongation in response to blue light. *Proc. Natl. Acad. Sci. USA* **113**, 224-229 (2016).
15. S. N. Gangappa, S. V. Kumar, DET1 and HY5 control PIF4-mediated thermosensory elongation growth through distinct mechanisms. *Cell Rep.* **18**, 344-351 (2017).
16. L. C. van der Woude, G. Perrella, B. L. Snoek, M. van Hoogdalem, O. Novak, M. C. van Verk, H. N. van Kooten, L. E. Zorn, R. Tonckens, J. A. Dongus, M. Praat, E. A. Stouten, M. C. G. Proveniers, E. Vellutini, E. Patitaki, U. Shapulatov, W. Kohlen, S. Balasubramanian, K. Ljung, A. R. van der Krol, S. Smeekens, E. Kaiserli, M. van Zanten, HISTONE DEACETYLASE 9 stimulates auxin-dependent thermomorphogenesis in *Arabidopsis thaliana* by mediating H2A.Z depletion. *Proc. Natl. Acad. Sci. USA* **116**, 25343-25354 (2019).
17. D. Ezer, J.H. Jung, H. Lan, S. Biswas, L. Gregoire, M. S. Box, V. Charoensawan, S. Cortijo, X. Lai, D. Stockle, C. Zubieta, K. E. Jaeger, P. A. Wigge, The evening complex coordinates environmental and endogenous signals in Arabidopsis. *Nat. Plant.* **3**, https://doi.org/10.1038/nplants.2017.87 (2017).
18. B. Thines, F. G. Harmon, Ambient temperature response establishes ELF3 as a required component of the core Arabidopsis circadian clock. *Proc. Natl. Acad. Sci. USA* **107**, 3257-3262 (2010).
19. C. Nieto, V. Lopez-Salmeron, J. M. Daviere, S. Prat, ELF3-PIF4 interaction regulates plant growth independently of the evening complex. *Curr. Biol.* **25**, 187-193 (2015).
20. S. F. Undurraga, M. O. Press, M. Legendre, N. Bujdoso, J. Bale, H. Wang, S. J. Davis, K. J. Verstrepen, C. Queitsch, Background-dependent effects of polyglutamine variation in the *Arabidopsis thaliana* gene *ELF3*. *Proc. Natl. Acad. Sci. USA* **109**, 19363-19367 (2012).
21. J. H. Jung, A. D. Barbosa, S. Hutin, J. R. Kumita, M. Gao, D. Derwort, C. S. Silva, X. Lai, E. Pierre, F. Geng, S. B. Kim, S. Baek, C. Zubieta, K. E. Jaeger, P. A. Wigge, A prion-like domain in ELF3 functions as a thermosensor inArabidopsis. *Nature* **585**, 256-260 (2020).
22. S. N. Gangappa, J. F. Botto, The BBX family of plant transcription factors. *Trend. Plant Sci.* **19**, 460-470 (2014).
23. L. Ding, S. Wang, Z. T. Song, Y. Jiang, J. J. Han, S. J. Lu, L. Li, J. X. Liu, Two B-box domain proteins, BBX18 and BBX23, interact with ELF3 and

regulate thermomorphogenesis in Arabidopsis. *Cell Rep.* **25**, 1718-1728 (2018).
24. J. W. Yu, V. Rubio, N. Y. Lee, S. Bai, S. Y. Lee, S. S. Kim, L. Liu, Y. Zhang, M. L. Irigoyen, J. A. Sullivan, Y. Zhang, I. Lee, Q. Xie, N. C. Paek, X. W. Deng, COP1 and ELF3 control circadian function and photoperiodic flowering by regulating GI stability. *Mol. Cell* **32**, 617-630 (2008).
25. W. J. Lyzenga, J. K. Booth, S. L. Stone, The Arabidopsis RING-type E3 ligase XBAT32 mediates the proteasomal degradation of the ethylene biosynthetic enzyme, 1-aminocyclopropane-1-carboxylate synthase 7. *Plant J.* **71**, 23-34 (2012).
26. S. D. Carvalho, R. Saraiva, T. M. Maia, I. A. Abreu, P. Duque, XBAT35, a novel Arabidopsis RING E3 ligase exhibiting dual targeting of its splice isoforms, is involved in ethyllene-mediated regulation of apical hook curvature. *Mol. Plant* **5**, 1295-1309 (2012).
27. H. Liu, S. Ravichandran, O. K. Teh, S. McVey, C. Lilley, H. J. Teresinski, C. Gonzalez-Ferrer, R. T. Mullen, D. Hofius, B. Prithiviraj, S. L. Stone, The RING-type E3 ligase XBAT35.2 is involved in cell death induction and pathogen response. *Plant Physiol.* **175**, 1469-1483 (2017).
28. L. A. Nodzon, W. H. Xu, Y. S. Wang, L. Y. Pi, P. K. Chakrabarty, W. Y. Song, The ubiquitin ligase XBAT32 regulates lateral root development in Arabidopsis. *Plant J.* **40**, 996-1006 (2004).
29. F. Yu, X. Cao, G. Liu, Q. Wang, R. Xia, X. Zhang, Q. Xie, ESCRT-I component VPS23A is targeted by E3 ubiquitin ligase XBAT35 for proteasome-mediated degradation in modulating ABA signaling. *Mol. Plant* **13**, 1556-1569 (2020).
30. W. M. Gray, A. Ostin, G. Sandberg, C. P. Romano, M. Estelle, High temperature promotes auxin-mediated hypocotyl elongation in Arabidopsis. *Proc. Natl. Acad. Sci. USA* **95**, 7197-7202 (1998).
31. E. Oh, J. Y. Zhu, Z. Y. Wang, Interaction between BZR1 and PIF4 integrates brassinosteroid and environmental responses. *Nat. Cell Biol.***14**, 802-809
32. T. Yamashino, Y. Nomoto, S. Lorrain, M. Miyachi, S. Ito, N. Nakamichi, C. Fankhauser, T. Mizuno, Verification at the protein level of the PIF4-mediated external coincidence model for the temperature-adaptive photoperiodic control of plant growth in Arabidopsis thaliana. *Plant Signal. Behav.* **8**, e23390 (2013).
33. M. S. Box, B. E. Huang, M. Domijan, K. E. Jaeger, A. K. Khattak, S. J. Yoo, E. L. Sedivy, D. M. Jones, T. J. Hearn, A. A. R. Webb, A. Grant, J. C. W. Locke, P. A. Wigge, ELF3 controls thermoresponsive growth in Arabidopsis. *Curr. Biol.* **25**, 194-199 (2015).

34. A. Raschke, C. Ibanez, K. K. Ullrich, M. U. Anwer, S. Becker, A. Gloeckner, J. Trenner, K. Denk, B. Saal, X. Sun, M. Ni, S. J. Davis, C. Delker, M. Quint, Natural variants of ELF3 affect thermomorphogenesis by transcriptionally modulating PIF4-dependent auxin response genes. *BMC Plant Biol.* **15**, 197 (2015).
35. Y. J. Park, H. J. Lee, J. H. Ha, J. Y. Kim, C. M. Park, COP1 conveys warm temperature information to hypocotyl thermomorphogenesis. *New Phytol.* **215**, 269-280 (2017).
36. J. J. Casal, Photoreceptor signaling networks in plant responses to shade. *Ann. Rev. Plant Biol.* **64***,* 403-427 (2013).
37. E. Herrero, E. Kolmos, N. Bujdoso, Y. Yuan, M. Wang, M. C. Berns, H. Uhlworm, G. Coupland, R. Saini, M. Jaskolski, A. Webb, J. Goncalves, S. J. Davis, EARLY FLOWERING4 recruitment of EARLY FLOWERING3 in the nucleus sustains the Arabidopsis circadian clock. *Plant Cell* **24**, 428-443 (2012).
38. A. Helfer, D. A. Nusinow, B. Y. Chow, A. R. Gehrke, M. L. Bulyk, S. A. Kay, LUX ARRHYTHMO encodes a nighttime repressor of circadian gene expression in the Arabidopsis core clock. *Curr. Biol.* **21**, 126-133 (2011).
39. C. S. Silva, A. Nayak, X. Lai, S. Hutin, V. Hugouvieux, J. H. Jung, I. Lopez-Vidriero, J. M. Franco-Zorrilla, K. C. S. Panigrahi, M. H. Nanao, P. A. Wigge, C. Zubieta, Molecular mechanisms of Evening Complex activity in Arabidopsis. *Proc. Natl. Acad. Sci. USA* **117**, 6901-6909 (2020).
40. R. Khanna, B. Kronmiller, D. R. Maszle, G. Coupland, M. Holm, T. Mizuno, S. H. Wu, The Arabidopsis B-box zinc finger family. *Plant Cell* **21**, 3416-3420 (2009).
41. L. Yan, S. Wei, Y. Wu, R. Hu, H. Li, W. Yang, Q. Xie, High-efficiency genome editing in Arabidopsis using YAO promoter-driven CRISPR/Cas9 system. *Mol. Plant* **8**, 1820-1823 (2015).
42. S. J. Clough, A. F. Bent, Floral dip: A simplified method for Agrobacterium-mediated transformation of *Arabidopsis thaliana*. *Plant J.* **16**, 735-743 (1998).

ACKNOWLEDGEMENTS

This project was financially supported by grants from the National Natural Science Foundation of China (numbers 31625004, 31872653 and 32000374), the Zhejiang Provincial Talent Program (2019R52005), the Natural Science Foundation of Zhejiang, China (LD21C020001), the 111 Project (B14027), and the BBSRC (BB/N018540/1). We would like to thank Profs. Qi Xie and Zuhua He for providing the constructs of E1, E2, and Ub for ubiquitination assays, and Profs. Hongtao Liu and Lei Wang for sharing the *phyA-211 phyB-9* mutant and *elf3-1* mutant seeds, respectively.

AUTHOR CONTRIBUTIONS

J.X.L. and L.L.Z. conceived and designed the experiments; L.L.Z., Y.J.S., L.D. and M.J.W. performed the experiments; J.X.L. and L.L.Z. analysed the data; J.X.L., S.J.D. and L.L.Z. wrote the article.

DECLARATION OF INTERESTS

The authors declare no competing interests.

DATA AVAILABILITY

All data needed to evaluate the conclusions in the paper are present in the paper and/or the Supplementary Materials.

SUPPLEMENTAL INFORMATION

Fig. S1 Independence of phytochromes on the warm temperature-induced up-regulation of *XBAT31*.

Wild-type and phytochrome mutants grown at 22°C were transferred to warm temperature (29°C) for 48 hr and sampled for RT-qPCR. Relative gene expression is the expression level of *XBAT31* relative to that in non-stressed WT plants, which was normalized to that of the internal control *PP2A*. Error bars

represent the SE (n=3). Letters above the bars indicate significant differences as determined by HSD test ($P < 0.05$).

Fig. S2 Targeted gene editing for *XBAT31*.

Sequences of XBAT31 derived from the WT and *XBAT31* mutant (*xbat31-1* and *xbat31-2)* plants are aligned. The mutated sites are highlighted in red. *, stop codon; ANK, ankry repeat; RING, Really Interesting New Gene.

Fig. S3 Hypocotyl growth of *XBAT31* mutants and overexpression plants in the dark.

Wild-type (WT), *XBAT31* mutant and overexpression plants were germinated and grown in the dark at 22°C for four days, after which the seedlings were imaged (A-B) and the hypocotyls were measured (C-D). The bars depict SD (n=24). Letters above the bars indicate significant differences as determined by Duncan's multiple range test ($P < 0.05$). Bar = 10 mm.

Fig. S4 Validation of transgene expression and antibody specific.

(**A-F**) Wild-type (WT), various mutant and transgenic plants were grown under respective conditions as described for phenotypic analysis. Total proteins were extracted for western blotting using specific antibodies. Tubulin was used as a loading control. (**G**) Total proteins were extracted from WT and *elf3-1* mutant plants grown at 22°C for western blotting using *anti*-ELF3 antibody. Equal amount of total proteins were loaded.

Fig. S5 Thermoresponsive expression of *ELF3* and *PIF4*.

WT, *xbat31-1* and *XBAT31ox-1* plants grown at 22°C were transferred to either 22°C or 29°C for 24 hr, and then sampled on the next day at different time points for gene expression analysis. The expression level of each sample was normalized to that in ZT 8 hr at 22°C, which was normalized to that of *PP2A*. The bars depict *SE* (n=3).

Fig. S6 Nuclear localization of XBAT31.

Full-length CDS of XBAT31 was fused to yellow fluorescent protein (YFP) at the C-terminus and expressed together with a nucleus marker (NLS-mCherry) in tobacco leaves. YFP empty vector was served as the control. After infiltration, tobacco leaves were observed using laser confocal microscopy (YFP channel) or light microscopy (bright field), after which both images were merged (overlay). Bar = 50 μm.

Fig. S7 Coomassie blue staining of protein gel for ubiquitination reaction. Purified GST-ELF3 was incubated with the native or mutated form of MBP-XBAT31 in the presence or absence of an E1, an E2 and an ubiquitin (Ub). MBP was used as a control. After the ubiquitination reaction, proteins were separated by SDS-PAGE and detected by Coomassie blue staining. The molecular weight (kDa) of the marker is indicated on the left side of the gel. *, unknown protein products related to GST-ELF3.

Table S1 | Primers used in this study.

FIGURE LEGENDS

Fig. 1 XBAT31 regulates thermomorphogenesis in Arabidopsis.

(**A-B**) Regulation of *XBAT31* expression by warm temperature. Wild-type (WT) seedlings grown at 22°C were transferred to either 22°C or 29°C and then the gene expression level was examined at different *Zeitgeber* Time (ZT) as indicated. (**C-F**) Phenotypes of *XBAT31* loss-of-function mutants and *XBAT31* overexpression plants. Seedlings of the WT, gene-edited mutant (*xbat31-1*/*xbat31-2*) and overexpression seedlings (*XBAT31ox-1*/*XBAT31ox-2*) grown at 22°C were transferred to either 22°C or 29°C for 3 days (E & F) or 4 days (C & D), after which representative plants were imaged (C & E) and the hypocotyl length was subsequently measured (D & F). Error bars depict *SD* (n=24). The *pif4-101* mutant was used as a control. Letters above the bars indicate significant differences as determined by HSD test ($P < 0.05$). Bar = 5 mm. (**G-H**) Differentially expression of thermoresponsive genes. WT, *xbat31-1* and *XBAT31ox-1* plants grown at 22°C were transferred to either 22°C or 29°C and then sampled at different ZT time points for gene expression analysis. The expression level of each sample was normalized to that in WT at ZT 8 hr at 22°C, which was normalized to that of *PP2A*. Error bars depict *SE* (n=3).

Fig. 2 Both *PIF4* and *ELF3* are epistatic to *XBAT31* in thermomorphogenesis.

(A-F) Genetic analysis of *PIF4* and *XBAT31* in thermomorphogenesis. The *pif4-101* and *xbat31-1* single mutants were crossed to generate the double mutant *xbat31-1 pif4-101* (A & D), while *PIF4* was overexpressed in the *xbat31-1* mutant background by crossing *PIF4ox-1* plants (WT background) to *xbat31-1* plants (B & E). *XBAT31* was overexpressed in the *pif4-101* mutant background by crossing *XBAT31ox-1* plants (WT background) to *pif4-101* plants (C & F). (**G-J**) Genetic analysis between *XBAT31* and *ELF3* in thermomorphogenesis. The *XBAT31ox-1* plants (WT background) and *ELF3ox-1* (WT background)

were crossed to generate the double overexpression plants (G & I), while the *xbat31-1 elf3-101* double mutant was obtained by crossing the respective single mutants (H & J). All the materials were firstly grown at 22°C and then transferred to either 22°C or 29°C for 4 days, after which representative plants were imaged and the hypocotyl length was subsequently measured. Error bars depict *SD* (n=24). The *pif4-101* mutant was used as a control. Letters above the bars indicate significant differences as determined by HSD test ($P < 0.05$). Bar = 5 mm.

Fig. 3 XBAT31 interacts with ELF3 both *in vitro* and *in vivo*.

(**A-D**) Protein-protein interaction between XBAT31 and ELF3 in yeast two-hybrid assays. The full-length (FL) and four truncations of XBAT31 (F1-F4) were fused with the DNA-binding domain (BD), while the full-length (FL), N-terminal (N), middle (M) and C-terminal (C) regions of ELF3 were fused with the activation domain (AD) of GAL4 (A-B). *HIS3* and *ADE2* were used for interaction reporters (C-D). (**E**) Pull-down assay. ELF3 was fused with a GST tag and XBAT31 was fused with a MBP tag. After co-incubation with both proteins, proteins were immuno-precipitated with glutathione-super-flow resins and detected using *anti*-MBP antibody. MBP was used as a negative control. (**F-G**) Split luciferase and split-YFP assays. XBAT31 and ELF3 were fused with the N-terminal (nLUC) and C-terminal (cLUC) portion of firefly luciferase, or the C-terminal (cYFP) and N-terminal (nYFP) portion of YFP, respectively. Empty vectors were used as controls. Different combinations of constructs were agro-infiltrated into tobacco leaves and the chemiluminescence or fluorescence was observed. Bar = 50 μm. (**H**) Co-immunoprecipitation (Co-IP) assays. Equal amount of total proteins from wild-type (WT) and *XBAT31* overexpression (*XBAT31-FLAG*) plants were immunoprecipitated with FLAG antibody-conjugated beads and detected using *anti*-ELF3 antibody.

Fig. 4 XBAT31 mediates the ubiquitination and degradation of ELF3 at warm temperature.

(**A-D**) ELF3 degradation in cell free degradation assays. Total proteins extracted from wild-type (WT) or *XBAT31* overexpression (*XBAT31ox-1*) seedlings were incubated with or without MG132 over the indicated time course, and the level of ELF3 was detected using *anti*-ELF3 antibody (A-B) and quantified (C-D). Tubulin was used as a loading control and CHX was used to inhibit protein synthesis. Error bars represent SE (n=3). *P < 0.05. (**E**) Ubiquitination of ELF3 by XBAT31 *in vitro*. GST-ELF3 was incubated with the native or mutated form of MBP-XBAT31 in the presence or absence of E1, E2 and ubiquitin (Ub). The ubiquitinated form of GST-ELF3 was detected using *anti*-Ub, *anti*-GST and *anti*-ELF3 antibodies, respectively. Brackets denote the ubiquitinated bands. (**F-I**) Regulation of ELF3 stability by XBAT31 *in vivo*. WT, *XBAT31ox-1* and *xbat31-1* seedlings grown at 22°C were transferred to 29°C, and ELF3 was checked with an *anti*-ELF3 antibody (F-G). Tubulin was used as a loading control. The band intensities in western blots were quantified (H-I). Error bars represent SE (n=3). Letters above the bars indicate significant differences as determined by HSD test (P < 0.05). The molecular weight (kDa) of the marker is indicated on the right side of the gel.

Fig. 5 XBAT31-mediated ELF3 degradation is dependent on BBX18.

(**A-F**) Requirement of *BBX18* for *XBAT31*-mediated thermomorphogenesis. *XBAT31* overexpression plant (*XBAT31ox-1*, WT background) was crossed to *bbx18-1* or *bbx23-1* or *bbx18-1 bbx23-1* mutant. *xbat31-1* was also crossed to *bbx18-1*. Seedlings grown at 22°C were transferred to either 22°C or 29°C for 4 days, after which representative plants were imaged (A-B). The hypocotyl length was subsequently measured (C-F). Error bars depict *SD* (n=24). Bar = 5 mm. (**G-I**) Protein-protein interaction between XBAT31 and BBX18 in the pull-down assay (G), split-luciferase assay (H) and split-YFP assay (I). MBP-BBX18

and GST-XBAT31 were incubated and immuno-precipitated with glutathione-super-flow resins, and detected using *anti*-MBP antibody (G). Different combinations of constructs were agro-infiltrated into tobacco leaves and the chemiluminescence or fluorescence was detected (H-I). Empty vectors were used as controls. Bar = 50 μm. (**J-M**) Dependence of *BBX18* for the XBAT31-regulated ELF3 stability. WT, *bbx18-1* mutant, *XBAT31ox-1* or *XBAT31ox-1 bbx18-1* plants grown at 22°C were transferred to 29°C, and ELF3 was checked with an *anti*-ELF3 antibody (J-K) and quantified (L-M). Tubulin was used as a loading control. Error bars represent SE (n=3). Letters above the bars indicate significant differences as determined by HSD test ($P < 0.05$).

Fig. 6 A simplified working model for XBAT31-mediated thermomorphogenesis in plants.

In this model, XBAT31 acts as an important regulator controlling the protein stability of ELF3 in Arabidopsis. Under normal ambient growth temperature conditions (e.g. 22°C), ELF3 functions as a negative regulator of PIF4 to inhibit hypocotyl elongation through either inhibiting the protein activity of PIF4 or inhibiting the expression of *PIF4*. Upon temperature elevation (*e.g.* 29°C), the E3 ubiquitin ligase XBAT31 interacts, ubiquitinates, and degrades ELF3, diminishing the inhibitory effect of ELF3 on PIF4, which promotes downstream gene expression (*e.g. YUC8*) and accelerates hypocotyl elongation. The warm temperature-responsive BBX protein BBX18 possibly functions as a scaffold protein to enhance XBAT31-mediated ELF3 degradation. Since ELF3 is an important component of EC, XBAT31 may also regulate protein stability of the entire EC under warm temperature conditions.

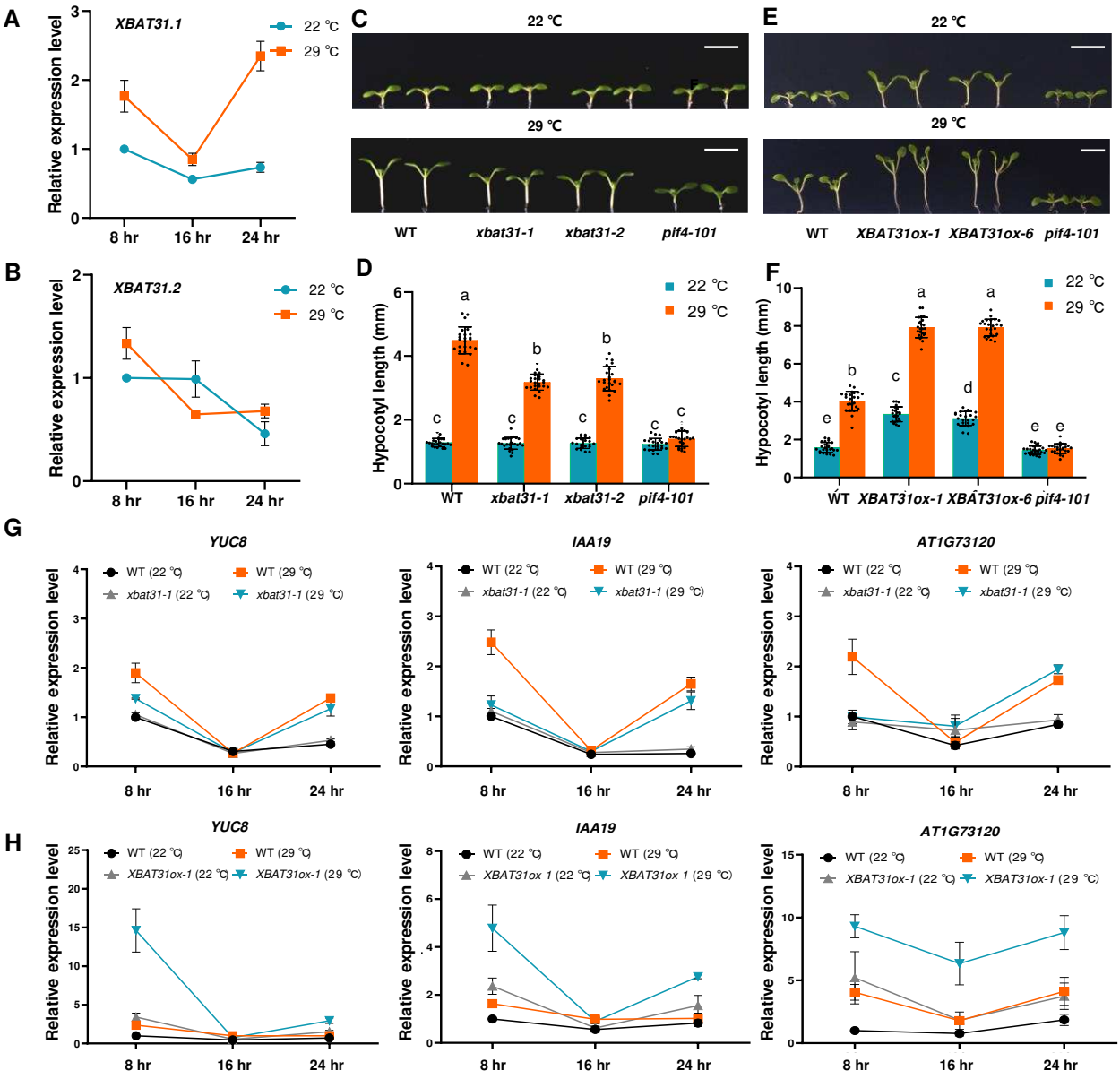

Fig. 1 XBAT31 regulates thermomorphogenesis in Arabidopsis.

(**A-B**) Regulation of *XBAT31* expression by warm temperature. Wild-type (WT) seedlings grown at 22° C were transferred to either 22° C or 29° C and then the gene expression level was examined at different *Zeitgeber* Time (ZT) as indicated. (**C-F**) Phenotypes of *XBAT31* loss-of-function mutants and *XBAT31* overexpression plants. Seedlings of the WT, gene-edited mutant (*xbat31-1*/*xbat31-2*) and overexpression seedlings (*XBAT31ox-1*/*XBAT31ox-2*) grown at 22° C were transferred to either 22° C or 29° C for 3 days (E & F) or 4 days (C & D), after which representative plants were imaged (C & E) and the hypocotyl length was subsequently measured (D & F). Error bars depict *SD* (n=24). The *pif4-101* mutant was used as a control. Letters above the bars indicate significant differences as determined by HSD test ($P < 0.05$). Bar = 5 mm. (**G-H**) Differentially expression of thermoresponsive genes. WT, *xbat31-1* and *XBAT31ox-1* plants grown at 22° C were transferred to either 22° C or 29° C and then sampled at different ZT time points for gene expression analysis. The expression level of each sample was normalized to that in WT at ZT 8 hr at 22° C, which was normalized to that of *PP2A*. Error bars depict *SE* (n=3).

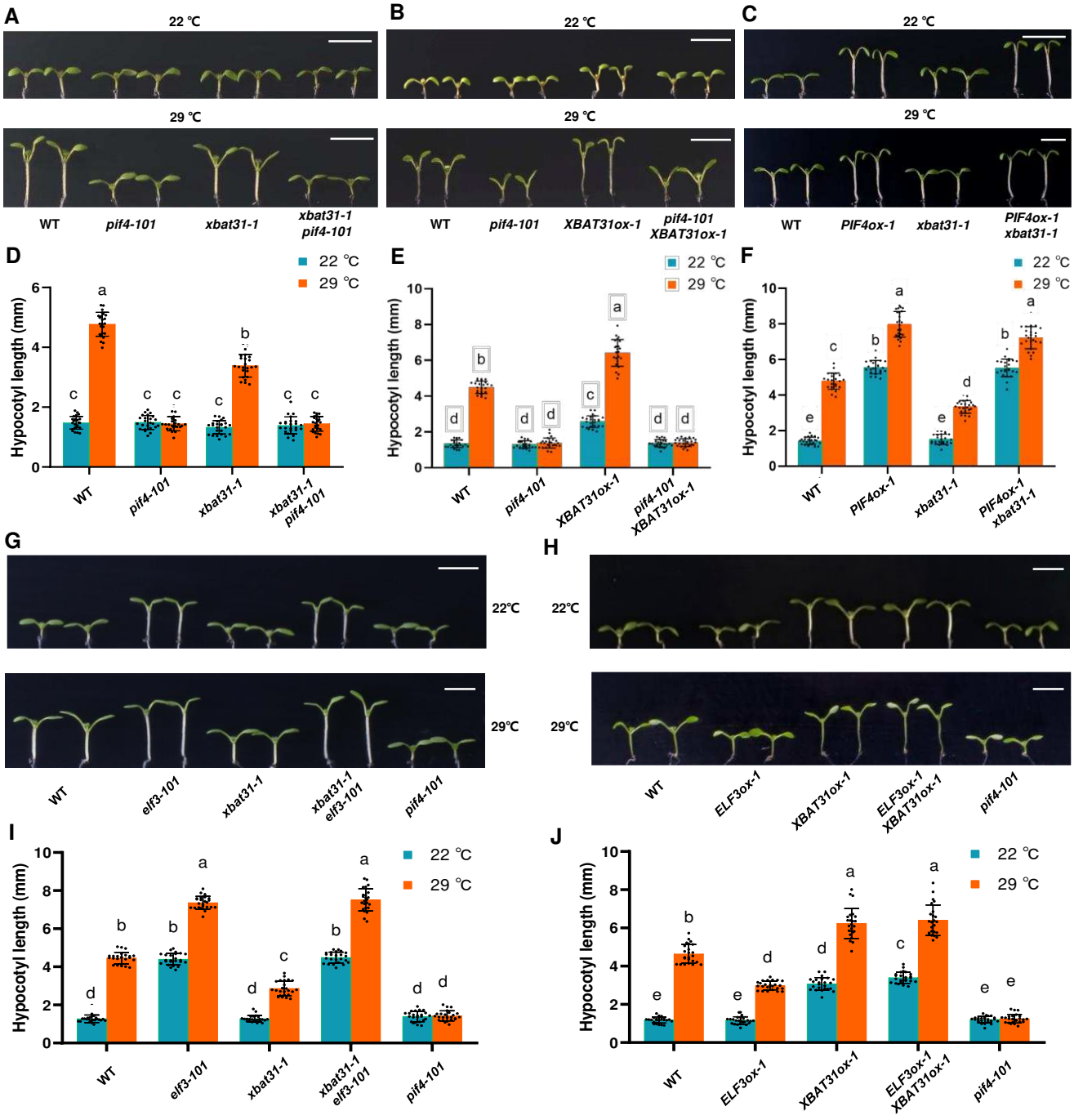

Fig. 2 Both *PIF4* and *ELF3* are epistatic to *XBAT31* in thermomorphogenesis.

(A-F) Genetic analysis of *PIF4* and *XBAT31* in thermomorphogenesis. The *pif4-101* and *xbat31-1* single mutants were crossed to generate the double mutant *xbat31-1 pif4-101* (A & D), while *PIF4* was overexpressed in the *xbat31-1* mutant background by crossing *PIF4ox-1* plants (WT background) to *xbat31-1* plants (B & E). *XBAT31* was overexpressed in the *pif4-101* mutant background by crossing *XBAT31ox-1* plants (WT background) to *pif4-101* plants (C & F). **(G-J)** Genetic analysis between *XBAT31* and *ELF3* in thermomorphogenesis. The *XBAT31ox-1* plants (WT background) and *ELF3ox-1* (WT background) were crossed to generate the double overexpression plants (G & I), while the *xbat31-1 elf3-101* double mutant was obtained by crossing the respective single mutants (H & J). All the materials were firstly grown at 22° C and then transferred to either 22° C or 29° C for 4 days, after which representative plants were imaged and the hypocotyl length was subsequently measured. Error bars depict *SD* (n=24). The *pif4-101* mutant was used as a control. Letters above the bars indicate significant differences as determined by HSD test ($P < 0.05$). Bar = 5 mm.

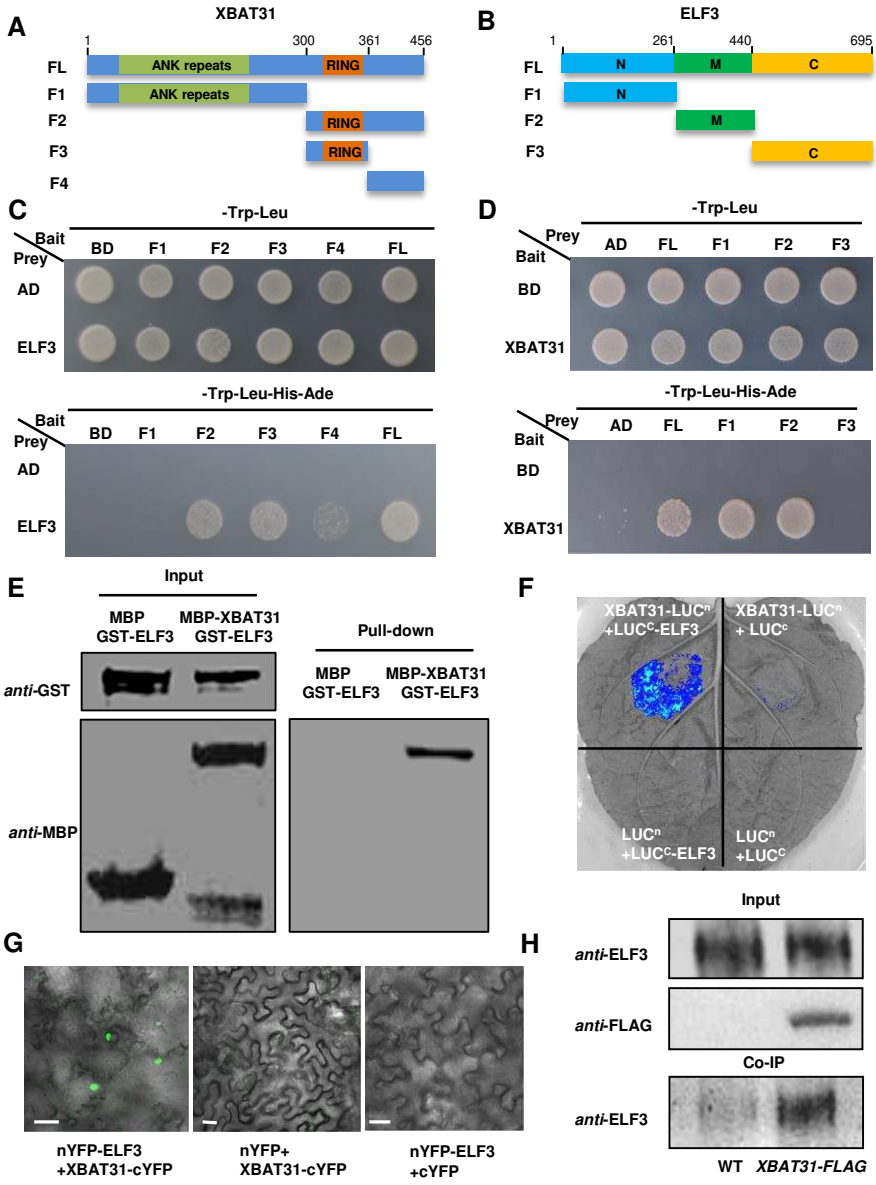

Fig. 3 XBAT31 interacts with ELF3 both *in vitro* and *in vivo*.

(**A-D**) Protein-protein interaction between XBAT31 and ELF3 in yeast two-hybrid assays. The full-length (FL) and four truncations of XBAT31 (F1-F4) were fused with the DNA-binding domain (BD), while the full-length (FL), N-terminal (N), middle (M) and C-terminal (C) regions of ELF3 were fused with the activation domain (AD) of GAL4 (A-B). *HIS3* and *ADE2* were used for interaction reporters (C-D). (**E**) Pull-down assay. ELF3 was fused with a GST tag and XBAT31 was fused with a MBP tag. After co-incubation with both proteins, proteins were immuno-precipitated with glutathione-super-flow resins and detected using *anti*-MBP antibody. MBP was used as a negative control. (**F-G**) Split luciferase and split-YFP assays. XBAT31 and ELF3 were fused with the N-terminal (nLUC) and C-terminal (cLUC) portion of firefly luciferase, or the C-terminal (cYFP) and N-terminal (nYFP) portion of YFP, respectively. Empty vectors were used as controls. Different combinations of constructs were agro-infiltrated into tobacco leaves and the chemiluminescence or fluorescence was observed. Bar = 50 μm. (**H**) Co-immunoprecipitation (Co-IP) assays. Equal amount of total proteins from wild-type (WT) and *XBAT31* overexpression (*XBAT31-FLAG*) plants were immunoprecipitated with FLAG antibody-conjugated beads and detected using *anti*-ELF3 antibody.

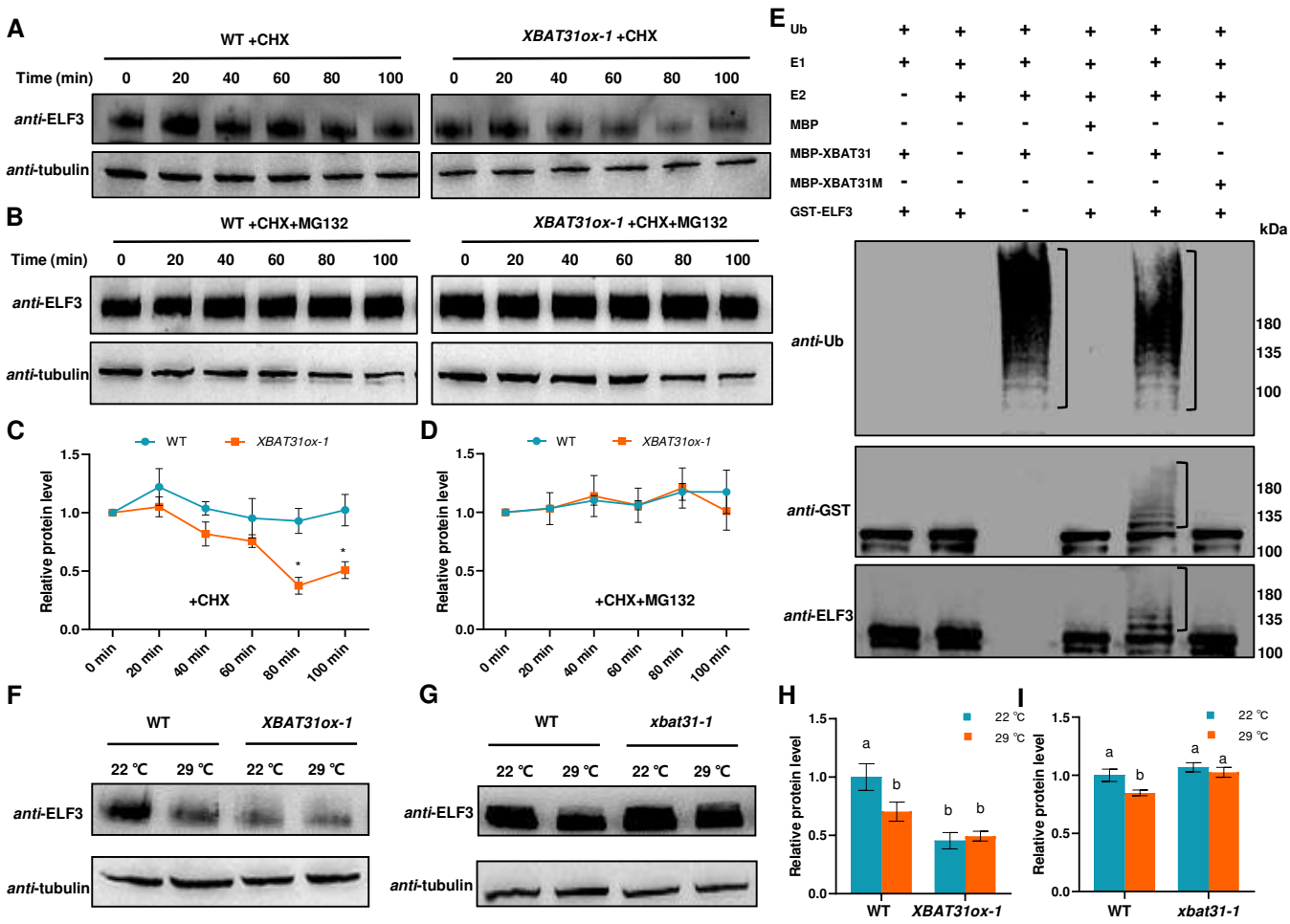

Fig. 4 XBAT31 mediates the ubiquitination and degradation of ELF3 at warm temperature.

(**A-D**) ELF3 degradation in cell free degradation assays. Total proteins extracted from wild-type (WT) or *XBAT31* overexpression (*XBAT31ox-1*) seedlings were incubated with or without MG132 over the indicated time course, and the level of ELF3 was detected using *anti*-ELF3 antibody (A-B) and quantified (C-D). Tubulin was used as a loading control and CHX was used to inhibit protein synthesis. Error bars represent SE (n=3). *P < 0.05. (**E**) Ubiquitination of ELF3 by XBAT31 *in vitro*. GST-ELF3 was incubated with the native or mutated form of MBP-XBAT31 in the presence or absence of E1, E2 and ubiquitin (Ub). The ubiquitinated form of GST-ELF3 was detected using *anti*-Ub, *anti*-GST and *anti*-ELF3 antibodies, respectively. Brackets denote the ubiquitinated bands. (**F-I**) Regulation of ELF3 stability by XBAT31 *in vivo*. WT, *XBAT31ox-1* and *xbat31-1* seedlings grown at 22° C were transferred to 29° C, and ELF3 was checked with an *anti*-ELF3 antibody (F-G). Tubulin was used as a loading control. The band intensities in western blots were quantified (H-I). Error bars represent SE (n=3). Letters above the bars indicate significant differences as determined by HSD test (P < 0.05). The molecular weight (kDa) of the marker is indicated on the right side of the gel.

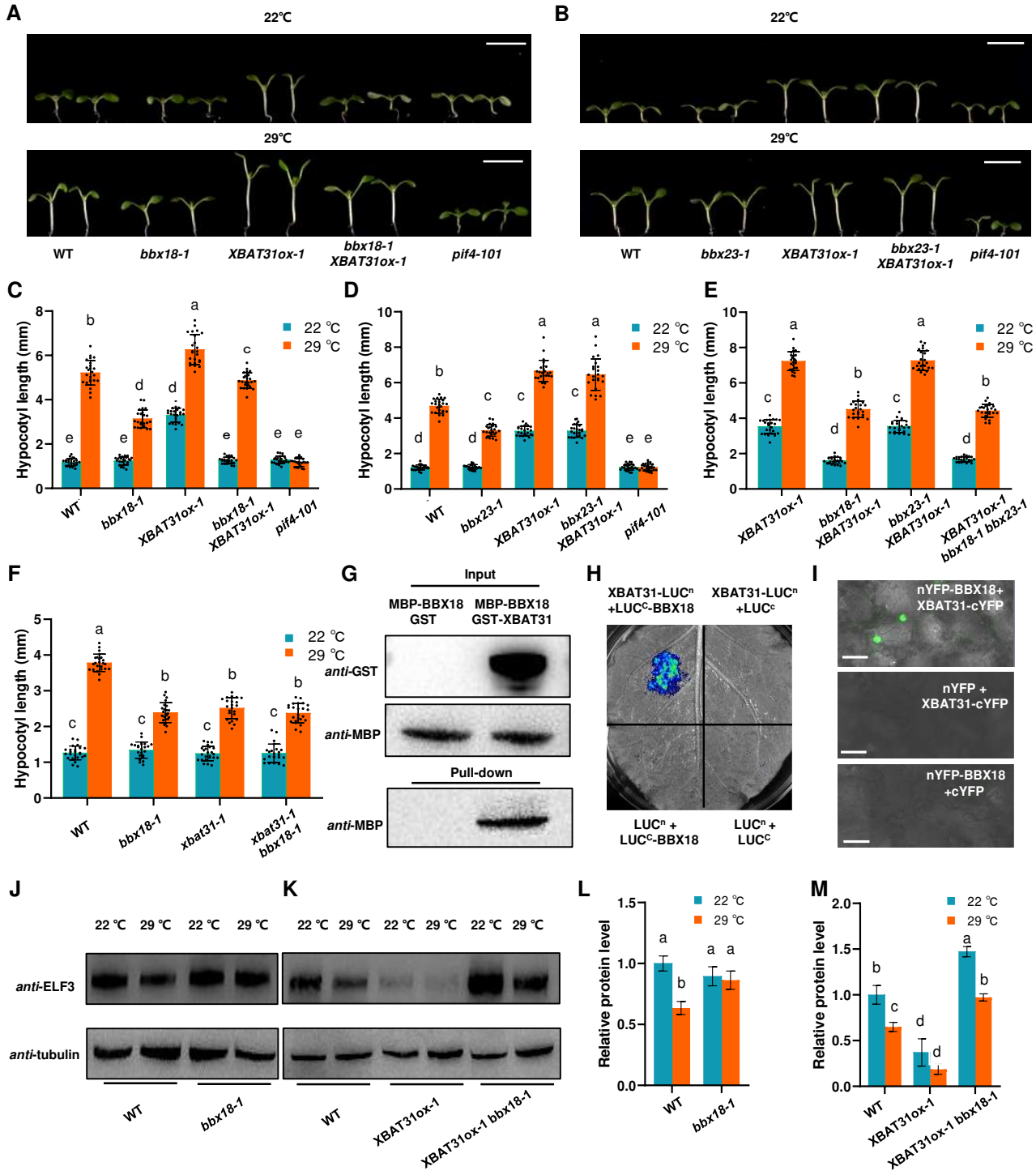

Fig. 5 XBAT31-mediated ELF3 degradation is dependent on BBX18.

(**A-F**) Requirement of *BBX18* for *XBAT31*-mediated thermomorphogenesis. *XBAT31* overexpression plant (*XBAT31ox-1*, WT background) was crossed to *bbx18-1* or *bbx23-1* or *bbx18-1 bbx23-1* mutant. *xbat31-1* was also crossed to *bbx18-1*. Seedlings grown at 22° C were transferred to either 22° C or 29° C for 4 days, after which representative plants were imaged (A-B). The hypocotyl length was subsequently measured (C-F). Error bars depict *SD* (n=24). Bar = 5 mm. (**G-I**) Protein-protein interaction between XBAT31 and BBX18 in the pull-down assay (G), split-luciferase assay (H) and split-YFP assay (I). MBP-BBX18 and GST-XBAT31 were incubated and immuno-precipitated with glutathione-super-flow resins, and detected using *anti*-MBP antibody (G). Different combinations of constructs were agro-infiltrated into tobacco leaves and the chemiluminescence or fluorescence was detected (H-I). Empty vectors were used as controls. Bar = 50 μm. (**J-M**) Dependence of *BBX18* for the XBAT31-regulated ELF3 stability. WT, *bbx18-1* mutant, *XBAT31ox-1* or *XBAT31ox-1 bbx18-1* plants grown at 22° C were transferred to 29° C, and ELF3 was checked with an *anti*-ELF3 antibody (J-K) and quantified (L-M). Tubulin was used as a loading control. Error bars represent SE (n=3). Letters above the bars indicate significant differences as determined by HSD test ($P < 0.05$).

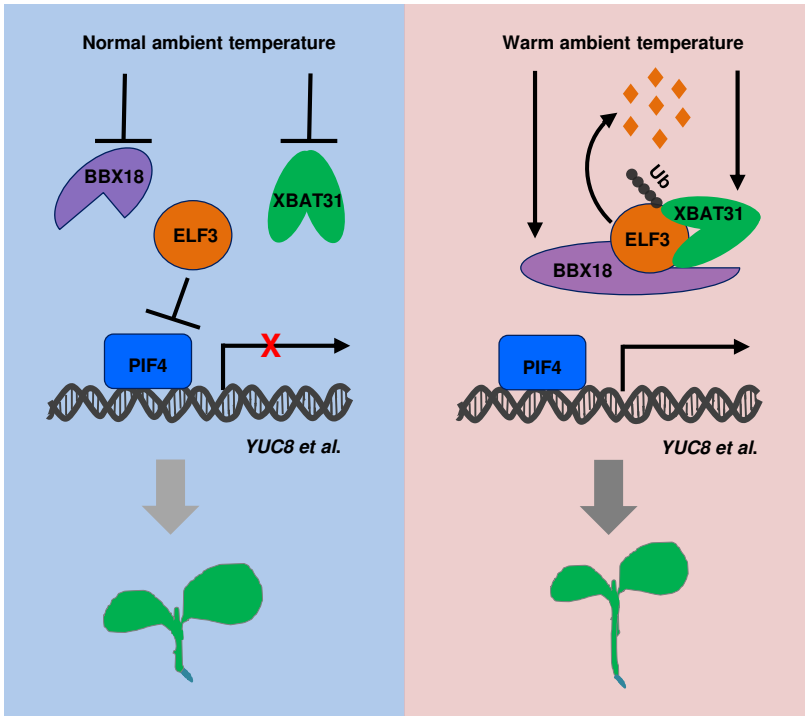

Fig. 6 A simplified working model for XBAT31-mediated thermomorphogenesis in plants.
In this model, XBAT31 acts as an important regulator controlling the protein stability of ELF3 in Arabidopsis. Under normal ambient growth temperature conditions (e.g. 22° C), ELF3 functions as a negative regulator of PIF4 to inhibit hypocotyl elongation through either inhibiting the protein activity of PIF4 or inhibiting the expression of *PIF4*. Upon temperature elevation (*e.g.* 29° C), the E3 ubiquitin ligase XBAT31 interacts, ubiquitinates, and degrades ELF3, diminishing the inhibitory effect of ELF3 on PIF4, which promotes downstream gene expression (*e.g. YUC8*) and accelerates hypocotyl elongation. The warm temperature-responsive BBX protein BBX18 possibly functions as a scaffold protein to enhance XBAT31-mediated ELF3 degradation. Since ELF3 is an important component of EC, XBAT31 may also regulate protein stability of the entire EC under warm temperature conditions.

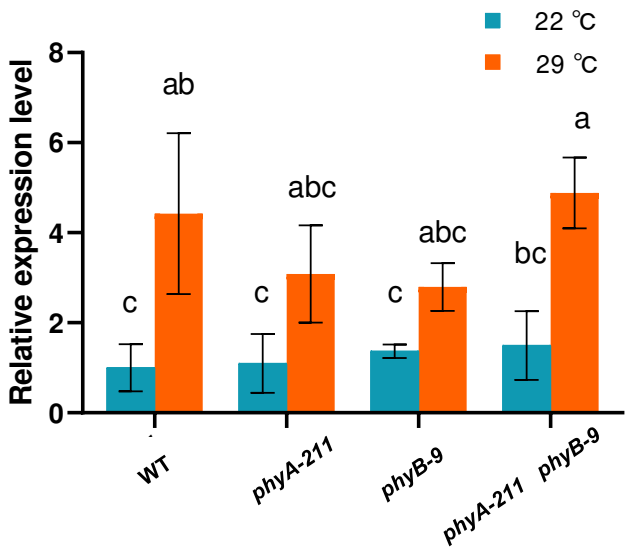

Fig. S1 Independence of phytochromes on the warm temperature-induced up-regulation of *XBAT31*.
Wild-type and phytochrome mutants grown at 22° C were transferred to warm temperature (29° C) for 48 hr and sampled for RT-qPCR. Relative gene expression is the expression level of *XBAT31* relative to that in non-stressed WT plants, which was normalized to that of the internal control *PP2A*. Error bars represent the SE (n=3). Letters above the bars indicate significant differences as determined by HSD test ($P < 0.05$).

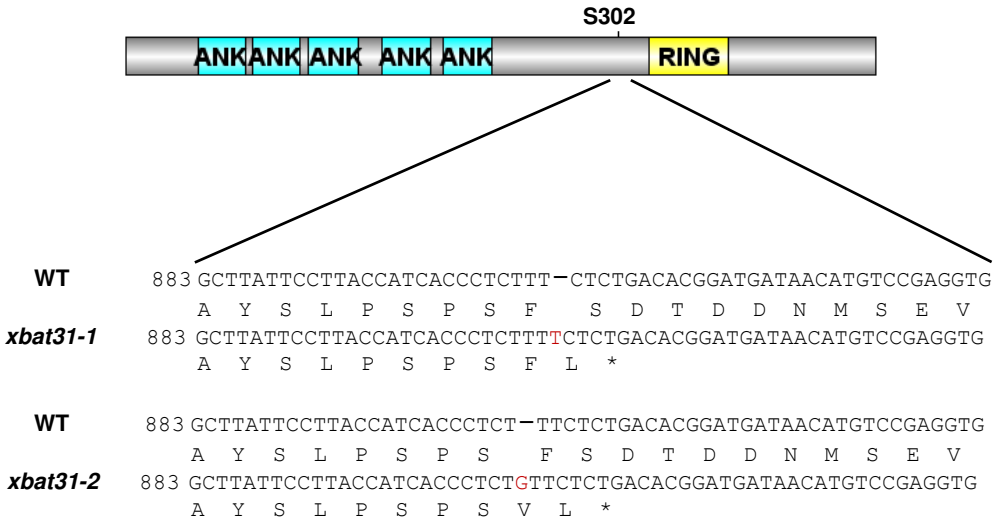

Fig. S2 Targeted gene editing for *XBAT31*.
Sequences of XBAT31 derived from the WT and *XBAT31* mutant (*xbat31-1* and *xbat31-2)* plants are aligned. The mutated sites are highlighted in red. *, stop codon; ANK, ankry repeat; RING, Really Interesting New Gene.

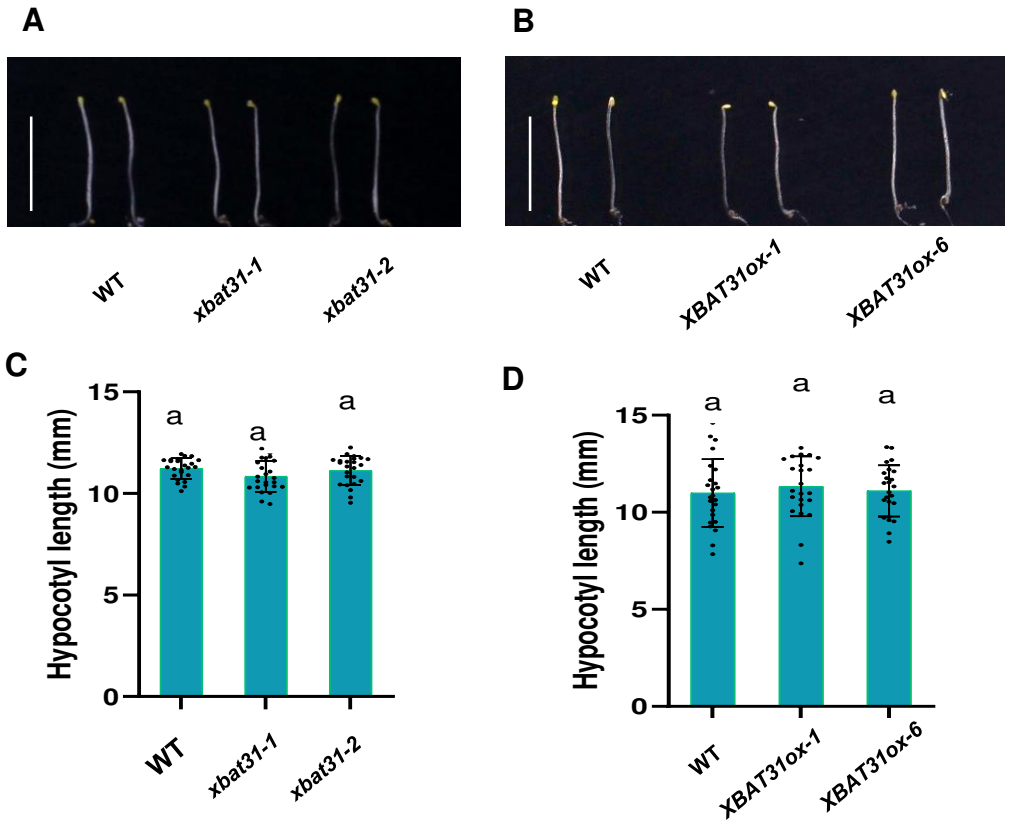

Fig. S3 Hypocotyl growth of *XBAT31* mutants and overexpression plants in the dark.
Wild-type (WT), *XBAT31* mutant and overexpression plants were germinated and grown in the dark at 22° C for four days, after which the seedlings were imaged (A-B) and the hypocotyls were measured (C-D). The bars depict SD (n=24). Letters above the bars indicate significant differences as determined by Duncan's multiple range test ($P < 0.05$). Bar = 10 mm.

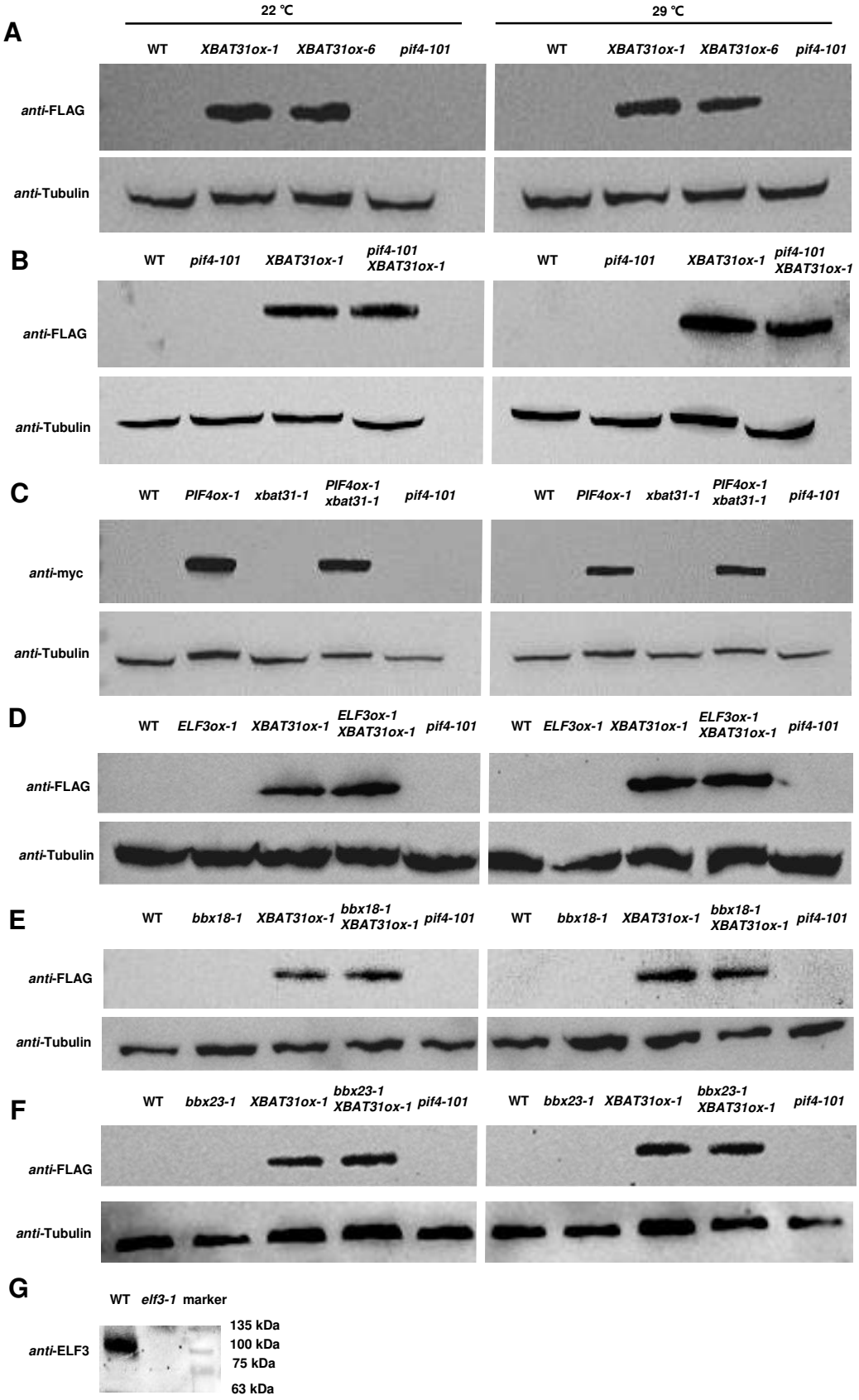

Fig. S4 Validation of transgene expression and antibody specific.

(**A-F**) Wild-type (WT), various mutant and transgenic plants were grown under respective conditions as described for phenotypic analysis. Total proteins were extracted for western blotting using specific antibodies. Tubulin was used as a loading control. (**G**) Total proteins were extracted from WT and *elf3-1* mutant plants grown at 22° C for western blotting using *anti*-ELF3 antibody. Equal amount of total proteins were loaded.

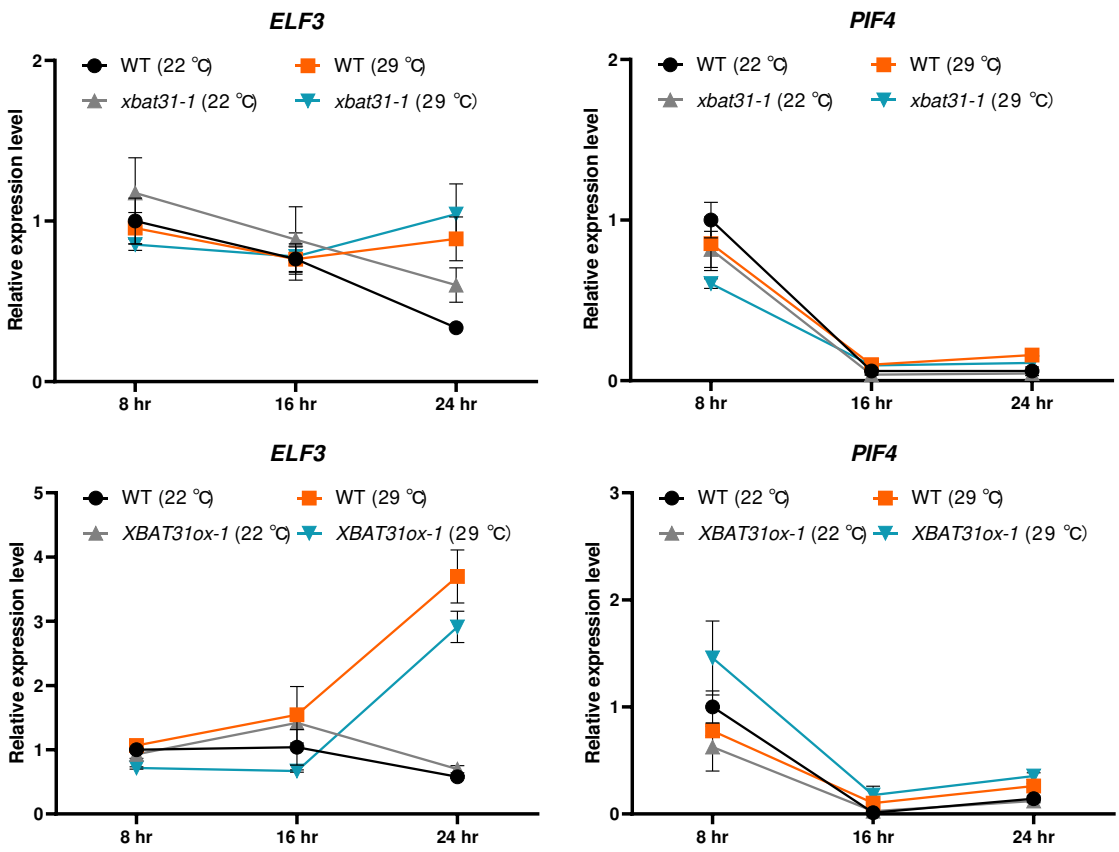

Fig. S5 Thermoresponsive expression of *ELF3* and *PIF4*.
WT, *xbat31-1* and *XBAT31ox-1* plants grown at 22° C were transferred to either 22° C or 29° C for 24 hr, and then sampled on the next day at different time points for gene expression analysis. The expression level of each sample was normalized to that in ZT 8 hr at 22° C, which was normalized to that of *PP2A*. The bars depict *SE* (n=3).

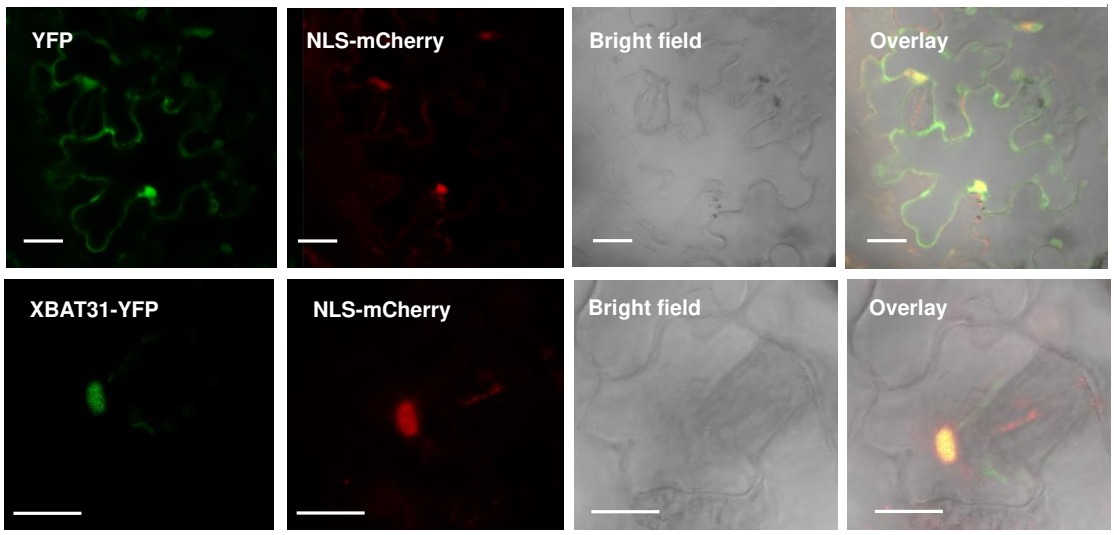

Fig. S6 Nuclear localization of XBAT31.
Full-length CDS of XBAT31 was fused to yellow fluorescent protein (YFP) at the C-terminus and expressed together with a nucleus marker (NLS-mCherry) in tobacco leaves. YFP empty vector was served as the control. After infiltration, tobacco leaves were observed using laser confocal microscopy (YFP channel) or light microscopy (bright field), after which both images were merged (overlay). Bar = 50 μm.

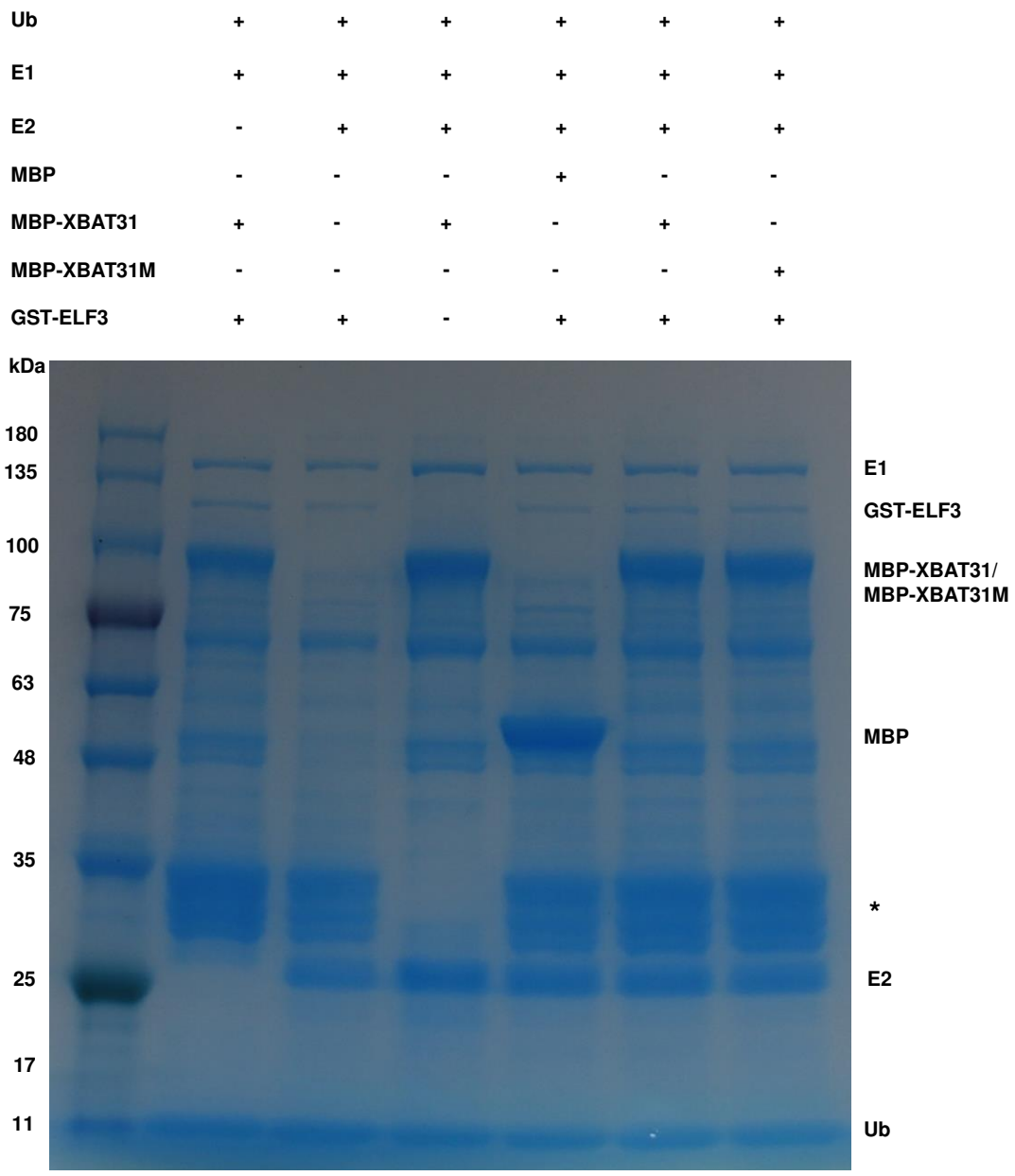

Fig. S7 Coomassie blue staining of protein gel for ubiquitination reaction. Purified GST-ELF3 was incubated with the native or mutated form of MBP-XBAT31 in the presence or absence of an E1, an E2 and an ubiquitin (Ub). MBP was used as a control. After the ubiquitination reaction, proteins were separated by SDS-PAGE and detected by Coomassie blue staining. The molecular weight (kDa) of the marker is indicated on the left side of the gel. *, unknown protein products related to GST-ELF3.

Table S1. Primers used in this Study

Name	Purpose	Forward Primer(5'-3')	Reverse Primer(5'-3')
sgXBAT31-t	sgRNA	ATTGTCATCCGTGTCAGAGAAAGA	AAACTCTTTCTCTGACACGGATGA
sgXBAT31-g	sgRNA	ATTGTCATCCGTGTCAGAGAAAGA	AAACTCTTTCTCTGACACGGATGA
ccXBAT31	Sequencing	TATGTGGTTGCGATGAAGCA	CGGGATCCTCACAATATTGGTTTGTCC
XBAT31-FLAG	Overexpression	GGGGTACCATGGGGCAGAGTATGAGCTG	CCCTCGAGCAATATTGGTTTGTCCATC
XBAT31-YFP	Localization	TTGGCGCGCCATGGGGCAGAGTATGAGCTG	CTAGTCTAGACAATATTGGTTTGTCCATC
XBAT31-nLUC	Split-LUC	GGGGTACCATGGGGCAGAGTATGAGCTG	CCCTCGAGCAATATTGGTTTGTCCATC
ELF3-cLUC	Split-LUC	CGGGATCCAATGAAGAGAGGGAAAGATGAGG	GCGTCGACTTAAGGCTTAGAGGAGTCATAGCG
BBX18-cLUC	Split-LUC	GGGGTACCATGCGAATTTTGTGTGATGC	GCGTCGACCTATTCATGCTCGTGATTG
XBAT31-cYFP	Split-YFP	CGGGATCCATGGGGCAGAGTATGAGCTG	CCGCTCGAGCAATATTGGTTTGTCCATC
nYFP-ELF3	Split-YFP	CGGGATCCATGAAGAGAGGGAAAGATGA	ACGCGTCGACTTAAGGCTTAGAGGAGTCAT
nYFP-BBX18	Split-YFP	CGGGATCCATGCGAATTTTGTGTGATGC	GCGTCGACCTATTCATGCTCGTGATTGT
BD-XBAT31	Y2H assay	CATGCCATGGAGATGGGGCAGAGTATGAGCTG	CCCTCGAGTCACAATATTGGTTTGTCC
BD-XBAT31-1	Y2H assay	CATGCCATGGAGATGGGGCAGAGTATGAGCTG	CCCTCGAGTGATGGTAAGGAATAAGCTG
BD-XBAT31-2	Y2H assay	CATGCCATGGAGCCCTCTTTCTCTGACACGGA	CCCTCGAGTCACAATATTGGTTTGTCC
BD-XBAT31-3	Y2H assay	CATGCCATGGAGCCCTCTTTCTCTGACACGGA	CCCTCGAGCAGAACGGACAGACCGGTGG
BD-XBAT31-4	Y2H assay	CATGCCATGGAGCCGGTCTGTCCGTTCTGTAG	CCCTCGAGTCACAATATTGGTTTGTCC
AD-ELF3-N	Y2H assay	TCCCCCGGGTATGAAGAGAGGGAAAGATGA	CCGCTCGAGGTGCCAAGTGAGATTCAGCTC
AD-ELF3-M	Y2H assay	TCCCCCGGGTGCAACGGAAAATCATTCACA	CCGCTCGAGGGTAGTTGGATTGTTGATGAT
AD-ELF3-C	Y2H assay	TCCCCCGGGTTACATGCCTTTTGCAAACAA	CCGCTCGAGGTTAAGGCTTAGAGGAGTCAT
MBP-BBX18	Purification	CGGGATCCATGCGAATTTTGTGTGATGC	GCGTCGACTTCATGCTCGTGATTGTTTGCG
MBP-XBAT31	Purification	CGGAATTCGATGGGGCAGAGTATGAGCTG	CGGGATCCTCACAATATTGGTTTGTCC
MBP-XBAT31RM-N	Purification	CGGAATTCGATGGGGCAGAGTATGAGCTG	GCACACATTTGGGCACCACAGTCT
MBP-XBAT31RM-C	Purification	AGACTGTGGTGCCCAAATGTGTGC	CGGGATCCTCACAATATTGGTTTGTCC
GST-ELF3	Purification	CGGGATCCATGAAGAGAGGGAAAGATGAGG	CCGCTCGAGTTAAGGCTTAGAGGAGTCATAGC
qXBAT31.1	qRT-PCR	CTGTTGAATCAAACTACTCC	GACGATTCAACAAATCTGGA
qXBAT31.2	qRT-PCR	ATCTCGTCGGAATCTGGTAT	TGCTTGTGACGATTCAACAA
qYUC8	qRT-PCR	TGTATGCGGTTGGGTTTACGAGGA	CCTTGAGCGTTTCGTGGGTTGTTT
qIAA19	qRT-PCR	GGTGACAACTGCGAATACGTTACCA	CCCGGTAGCATCCGATCTTTTCA
qAT1G73120	qRT-PCR	ATGGCGACTTCTACCTTCTC	TCCGGAGCTAGAGCCCTCAG
qELF3	qRT-PCR	TCCAGCATAGATGTCTCTCC	GTAGAGGAGGCTTTACCAGA
qPIF4	qRT-PCR	GCCTAAGGCCTGTCCTGA	GACATCGAGATCGTTCTGTG
qPP2A	qRT-PCR	TAACGTGGCCAAAATGATGC	GTTCTCCACAACCGCTTGGT